

TOOLS AND RESOURCES

Genetic knockdown of genes that are obscure, conserved and essential using CRISPR interference methods in the fission yeast *S. pombe*

Ken Ishikawa*, Saeko Soejima and Shigeaki Saitoh*

ABSTRACT

Characterizing functions of essential genes is challenging, as perturbing them is generally lethal. Conditional gene perturbation, including use of temperature-sensitive mutants, has been widely utilized to reveal functions of essential genes in the fission yeast *Schizosaccharomyces pombe*. However, recently we implemented a systematic and less time-consuming knockdown method, CRISPR interference (CRISPRi), in this organism using catalytically inactive Cas9 (dCas9). This technology has been expected to facilitate characterization of essential genes in *S. pombe*, although this still has not occurred. Here, CRISPRi was harnessed to study uncharacterized essential genes that are evolutionally conserved from yeasts to mammals. Transcription of these genes, which we call conserved essential obscure (*ceo*) genes, was repressed using conventional dCas9-mediated CRISPRi and by implementing technologies that enhance repression efficiency or alleviate limitations on small guide RNA (sgRNA) design. These CRISPRi methods successfully reduced transcription of target genes and allowed us to characterize resulting phenotypes. Knockdown of *ceo* genes inhibited cell proliferation and altered cellular morphology. Thus, dCas9-based CRISPRi methods utilized in this study enhanced accessibility of genetic analyses targeting essential genes in *S. pombe*.

KEY WORDS: Knockdown, Essential gene, CRISPR-Cas, CRISPRi, dCas9, Fission yeast, Biotechnology

INTRODUCTION

CRISPR-Cas (for ‘clustered regularly interspaced short palindromic repeat–CRISPR-associated’) is a form of adaptive immunity that restricts viral infection in bacteria and archaea (Knott and Doudna, 2018). In laboratories, artificial type II CRISPR-Cas system cleave specific target DNAs with a ribonucleoprotein complex comprising the Cas9 DNA endonuclease and small guide RNA (sgRNA). sgRNA has a targeting sequence (formally called a spacer sequence), which is a 20–30-nt sequence complementary to a specific target DNA (Jinek et al., 2012). The Cas9 ribonucleoprotein complex recognizes a specific target DNA through two mechanisms, Watson–Crick base-pairing with the targeting/spacer sequence by the sgRNA, and 2–5-bp PAM


(protospacer adjacent motif) sequence recognition by Cas9 protein (PAM is situated immediately to the 3’-side of the targeted, protospacer DNA sequence) (Sternberg et al., 2014).

Given that this artificial CRISPR-Cas system contains only *cas9* and sgRNA genes, it is easily manipulated so as to cleave arbitrary target DNAs by altering the targeting sequence encoded by the sgRNA gene; therefore, Cas9 and sgRNA are utilized for genome editing in a broad range of organisms, including *Schizosaccharomyces pombe* (Hayashi and Tanaka, 2019; Jacobs et al., 2014; Rodríguez-López et al., 2016; Zhang et al., 2018). In addition to genome editing, this artificial system is utilized for transcriptional alteration. Catalytically inactive Cas9 (dCas9) retains specific DNA-binding activity, and its binding to specific DNA targets can inhibit transcription there (Bikard et al., 2013; Qi et al., 2013). This technology, CRISPR interference (CRISPRi), was originally established using bacterial systems, and later implemented in many other organisms. For fission yeast, Zhao and Boeke established Cas12a (class 2 type V system)-mediated CRISPRi (Zhao and Boeke, 2020), and we recently implemented the Cas9-mediated method (Ishikawa et al., 2021). Transcriptional repression efficiency of CRISPRi is affected by the position at which dCas9 binds to the target DNA, and the effective binding position differs for each organism (Bikard et al., 2013; Gilbert et al., 2014; Lawhorn et al., 2014; McGlincy et al., 2021; Qi et al., 2013). We revealed that in *S. pombe*, complementary binding by the targeting sequence to either non-template strand at the transcription initiation (start) site (TSS) of a target gene or template strand 60–120 bp downstream of the TSS is preferred for efficient transcriptional repression by dCas9-mediated CRISPRi (Ishikawa et al., 2021). This rule for selecting targeting sequences can dramatically reduce the labor needed to design effective sgRNAs for dCas9-mediated CRISPRi in *S. pombe*.

The fission yeast *S. pombe* is a well-studied model organism. Genetic analyses using it have revealed numerous conserved gene functions among eukaryotes. However, characterizing genes essential for cellular viability is still challenging, given that perturbing functions of essential genes causes cell death. Thus, construction of strains defective in essential genes is not feasible. Physiological functions of essential genes have traditionally been analyzed using conditionally defective mutants, such as temperature-sensitive mutants, but these are not always available. Although recently developed methods, such as forced protein degradation, promoter replacement and 3’ untranslated region (3’ UTR) disruption, enable researchers to reduce expression and function of target genes without using conditionally defective mutations, these methods are time-consuming, as they require modification of genomic DNA sequences of target genes (Bähler et al., 1998; Kanke et al., 2011; Roguev et al., 2008; Schuldiner et al., 2005). CRISPRi is another feasible option to conditionally

Department of Cell Biology, Institute of Life Science, Kurume University, Asahi-machi 67, Kurume, Fukuoka 830-0011, Japan.

*Authors for correspondence (ishikawa_ken@kurume-u.ac.jp; saitoh_shigeaki@kurume-u.ac.jp)

 K.I., 0000-0003-4645-4422; S. Saitoh, 0000-0001-5408-296X

Handling Editor: Maria Carmo-Fonseca
Received 28 March 2023; Accepted 1 April 2023

repress transcription of target genes. In contrast to other methods, dCas9-mediated CRISPRi can be executed simply by introducing a plasmid harboring a sgRNA gene and the *dCas9* gene into *S. pombe* cells and inducing expression of dCas9 (Fig. 1A). In the plasmid, pSPdCas9, the *dCas9* gene is placed under the regulatable promoter, *nmt1-41p*. Genes can be knocked down arbitrarily using this method at desired timing, as long as a proper sgRNA is designed (Ishikawa et al., 2021). Owing to such simplicity of implementation, dCas9-mediated CRISPRi is potentially suitable for systematic functional analyses of essential genes in *S. pombe*. However, to our knowledge, this technology had not been utilized for this purpose.

Here, we successfully improved dCas9-mediated CRISPRi in fission yeast to achieve more efficient transcriptional repression and broader options for sgRNA design. Using the original and improved versions of CRISPRi, we then systematically knocked down seven genes that are evolutionarily conserved from yeasts to mammals but have not been well characterized. This allowed us to investigate phenotypes that emerged after their perturbation in *S. pombe*. CRISPRi is thus a feasible option to study physiological roles of essential genes for which conditional mutant strains are not available.

RESULTS

Simultaneous application of two sgRNAs for a single target gene greatly enhances transcriptional repression efficiency of CRISPRi

Although conventional CRISPRi, which consists of dCas9 protein and an sgRNA against a target gene, can repress transcription of a

model gene, *ade6⁺*, by as much as ~85% in *S. pombe* (Ishikawa et al., 2021), simultaneously applying two distinct sgRNAs against a single target gene reportedly increased transcriptional repression efficiency of CRISPRi in *E. coli* (Qi et al., 2013). This is called double sgRNA repression. As each fission yeast gene has two distinct spots potentially suitable for sgRNAs in close proximity to the TSS and 60–120 bp downstream (Ishikawa et al., 2021), by targeting both spots, we examined whether double sgRNA repression can enhance transcriptional repression by CRISPRi in this organism. To implement double sgRNA repression for fission yeast, we constructed a plasmid that has two sgRNA units in addition to a dCas9 gene placed under the thiamine-repressible *nmt1-41p* promoter (Fig. 1B, pSPdCas9.5). We then inserted two effective targeting sequences, ‘a5’ and ‘a10’, into the sgRNA units on this plasmid. Sequence a5 binds in the vicinity of the TSS of the *ade6⁺* gene, whereas a10 binds downstream of the TSS (Fig. 2A). The resulting plasmids, pSC5(a5,a10) and pSC5(a10,a5), were introduced to perform double sgRNA repression of *ade6⁺* gene expression.

In cells harboring a plasmid containing either a5 or a10 sgRNA [pSC2(a5), pSC2(a10), pSC5(a5,ns) or pSC5(ns,a5)], levels of *ade6⁺* mRNA decreased to ~16% of that in control cells with a nonsense sgRNA (ns), consistent with results previously reported (Ishikawa et al., 2021) (Fig. 2B). In cells harboring a plasmid expressing both a5 and a10 sgRNAs simultaneously [pSC5(a5,a10) and pSC5(a10,a5)], *ade6⁺* mRNA abundance was further reduced to 8–9% of the control, indicating that double sgRNA repression reduced the *ade6⁺* mRNA level by half in comparison with conventional CRISPRi using a single sgRNA. In cells with

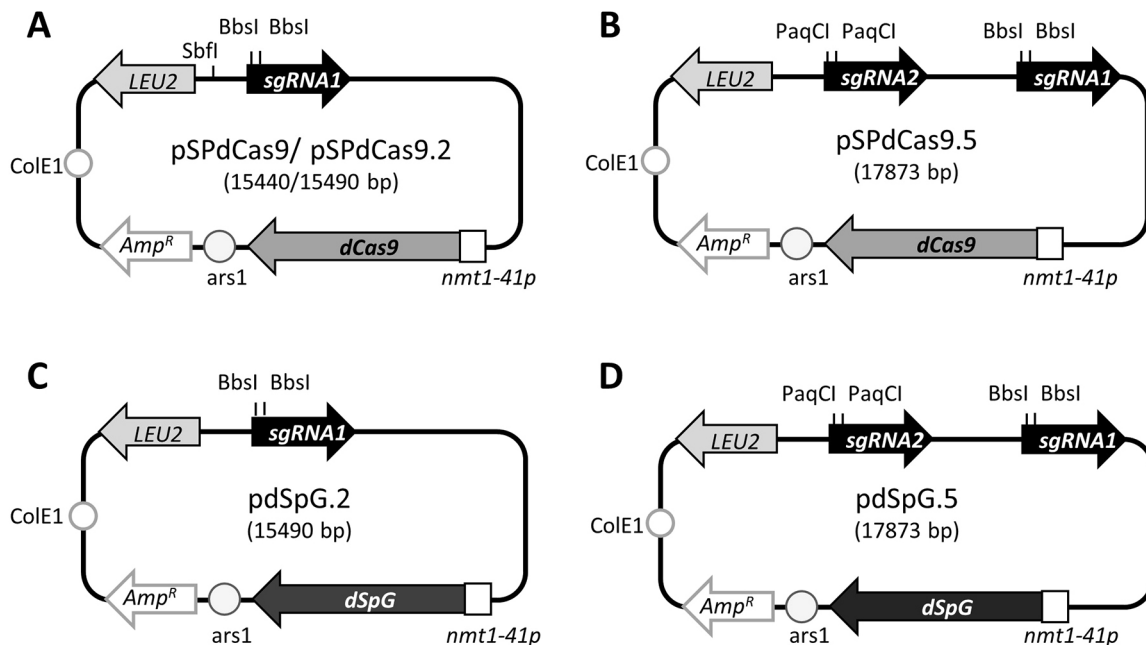


Fig. 1. Plasmids to induce dCas9-mediated CRISPRi in *S. pombe*. (A) Plasmid map of pSPdCas9 and pSPdCas9.2. pSPdCas9.2 has PmeI and BamHI restriction sites inserted at the SbfI indicated site (see Materials and Methods). (B) pSPdCas9.5 for double sgRNA repression. (C) pdSpG.2 for dSpG-mediated CRISPRi. (D) pdSpG.5 for dSpG-mediated double repression. dCas9, humanized dCas9, originally from *Streptococcus pyogenes*. dSpG, an artificial variant of dCas9, that has relaxed specificity of PAM. *nmt1-41p*, a moderate-strength variant of the *nmt1* promoter, transcription of which is inducible. *ars1*, a DNA replication origin of the *S. pombe*; *Amp^R*, ampicillin resistance gene; ColE1, DNA replication origin for *E. coli*; *LEU2*, the budding yeast leucine biogenesis gene that complements defects of the *leu1* gene in fission yeast; sgRNA1, the sgRNA gene, the targeting sequence of which can be replaced with an arbitrary DNA sequence at BbsI cleavage sites. sgRNA2, the sgRNA gene, the targeting sequence of which can be replaced with an arbitrary DNA sequence at PaqCI cleavage sites. When the targeting sequence is not replaced, these plasmids express one or two sgRNA(s) with a nonsense targeting sequence(s).

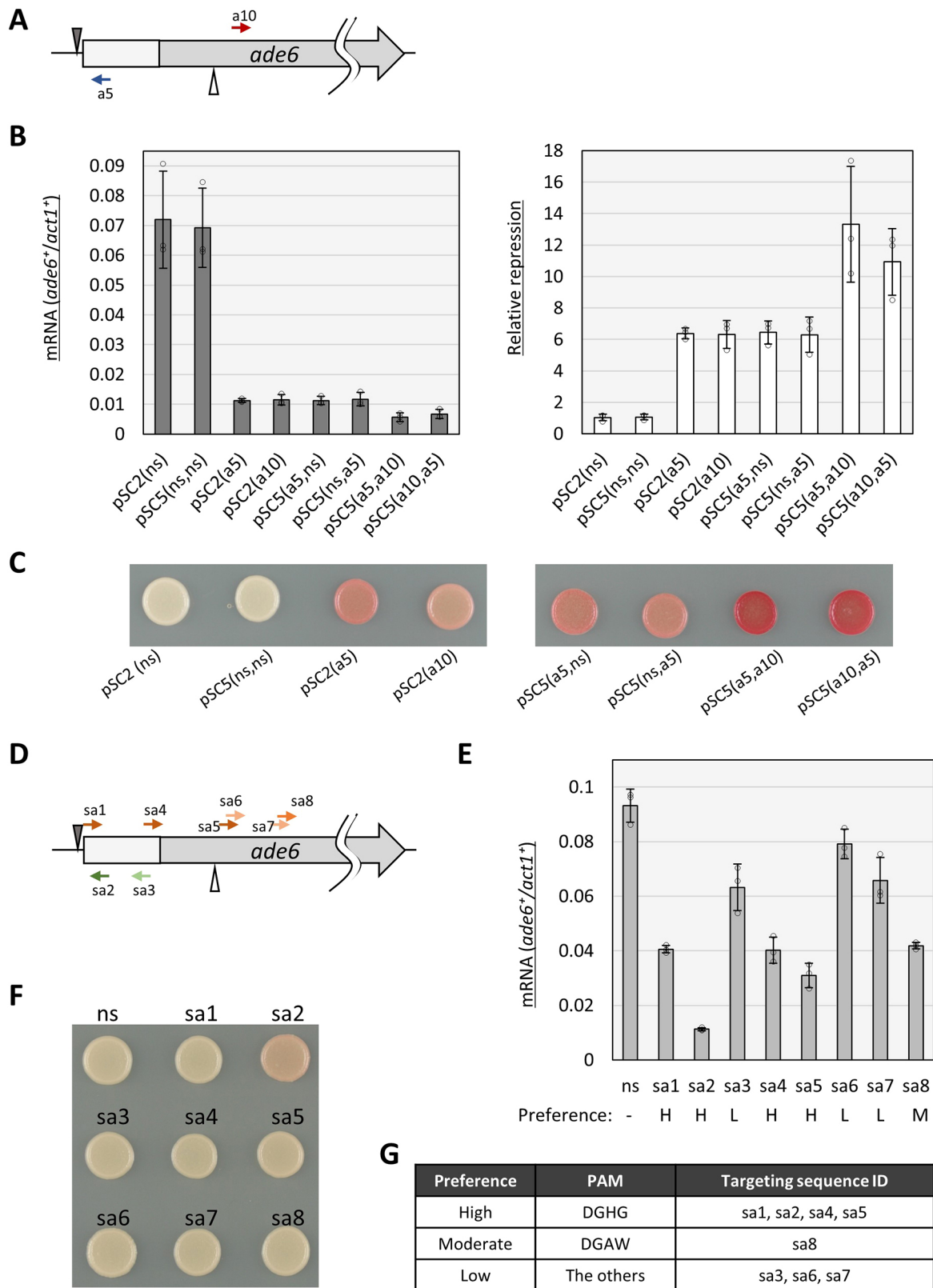


Fig. 2. See next page for legend.

reduced *ade6*⁺ gene expression, colonies became reddish due to accumulation of a red pigment, 5-aminoimidazole ribotide, which is an intermediate of adenine biosynthesis (Fig. 2C). Consistent with lower expression of *ade6*⁺, the colony color of cells subjected to

double sgRNA repression was darker than of cells subjected to conventional CRISPRi with a single sgRNA. Greatly enhanced transcriptional repression efficiency by CRISPRi by double sgRNA repression in *S. pombe* was thus confirmed.

Fig. 2. Implementation of the double sgRNA repression and dSpG-mediated CRISPRi in *S. pombe*. (A) Designed targeting sequences for dCas9-mediated CRISPRi of the *ade6⁺* gene. Red and blue arrows indicate targeting sequences of sgRNAs that base-pair with the template and non-template strands of the targeted DNA, respectively. PAM sequences are situated at the immediate 3'-side of the arrowheads (not shown in the diagram). Gray triangle, TSS; white triangle, the position 90 bp downstream from the TSS; light gray box, 5'UTR. (B) Left, quantification of *ade6⁺* mRNA. mRNA of *ade6⁺* and *act1⁺* was quantified by RT-qPCR. Relative mRNA amounts of *ade6⁺* normalized by that of *act1⁺* are presented. Right, repression efficiency. Reciprocal numbers of transcription level relative to the control are presented as the repression efficiency. Quantitative data show means \pm s.d. from three biological replicates. ns, nonsense targeting sequence; open circle, individual data point. (C,F) Color assay of *ade6⁺* expression. Yeast cell cultures after CRISPRi induction were spotted on a low-adenine medium. Images representative of three biological repeats. (D) Targeting sequences designed for dSpG-mediated CRISPRi of the *ade6⁺* gene. Orange and green arrows indicate targeting sequences of sgRNAs that base-pair with the template and non-template strands of the targeted DNA, respectively. (E) Quantification of *ade6⁺* mRNA. mRNA of *ade6⁺* and *act1⁺* as determined by RT-qPCR. Relative mRNA amounts of *ade6⁺* normalized by that of *act1⁺* are presented. Data show means \pm s.d. from three biological replicates. H, M, and L indicates preference of PAM by dSpG (H, high; M, moderate; L, low). ns, nonsense targeting sequence; open circle, individual data point. (G) PAM classification of preference by SpG based on a previous report (Walton et al., 2020). D (=A, G, T), H (=A, C, T), W (=A, T).

Utilization of a dCas9 variant with relaxed PAM specificity expands availability of targeting sequences suitable for CRISPRi

The PAM sequence, which is recognized by Cas9 protein, is a main limitation for designing sgRNAs. The dCas9 utilized in our CRISPRi method is derived from *Streptococcus pyogenes*. The PAM of *S. pyogenes* Cas9 is 5'-NGG (N=A, C, G or T) (Jinek et al., 2012). Therefore, targeting sequences for dCas9-mediated CRISPRi must be located right next to this sequence motif. Although a reverse targeting sequence binding at the TSS of a target gene and a forward targeting sequence binding ~90 bp downstream of the TSS are most preferable for transcriptional repression by dCas9-mediated CRISPRi in *S. pombe* (Ishikawa et al., 2021), targeting sequences are not always available at such positions because of the limitation imposed by the PAM sequence. Recently, a variant of Cas9 that recognizes relaxed PAM sequences, 5'-NGN, was artificially created, and successfully applied to genome and base editing (Walton et al., 2020). To investigate whether this variant, designated as SpG, is also suitable for CRISPRi, we generated plasmids pdSpG.2 and pdSpG.5 in which nucleotide changes of the SpG were introduced to the dCas9 gene (Fig. 1C,D). Eight targeting sequences were designed at the illustrated positions in the *ade6⁺* gene (Fig. 2D), inserted into the sgRNA cassette of pdSpG.2, and resulting plasmids were introduced into *S. pombe* cells for evaluation of their transcriptional repression capacity (Fig. 2E,F). Among targeting sequences tested (sa1–sa8), sa2, which binds to the non-template strand in the vicinity of the TSS, showed the most effective repression. In this strain, the *ade6⁺* mRNA level was reduced to 12.1% of the control (Fig. 2E), and cells formed reddish colonies (Fig. 2F). These results indicate that dSpG-mediated CRISPRi is as effective as dCas9-mediated CRISPRi, and that it is particularly useful in cases in which targeting sequences linked to canonical PAM sequences for dCas9, 5'-NGG, are not found in regions preferred for transcriptional repression.

Notably, dSpG is not equally effective for targets with each sequence of the 5'-NGN (Walton et al., 2020). Consistent with a previous report (Walton et al., 2020), PAM sequences of 5'-DGHG

(D=A, G or T; H=A, C or T) yielded the most effective transcriptional repression of the *ade6⁺* gene (Fig. 2E,G). These results confirmed that the preferred PAM sequences (5'-DGHG) should be chosen for effective CRISPRi with the dSpG. Although dSpG provides additional variation of PAM sequences available for CRISPRi, targets with 5'-NGG PAM still have to be repressed by dCas9 rather than dSpG, given that some options of 5'-NGG are not preferred by SpG (Walton et al., 2020) (Fig. S1).

Systematic knockdown of conserved essential obscure genes

S. pombe is an excellent unicellular model organism to study molecular and physiological functions of evolutionarily conserved genes. Among 1221 essential genes, deletion of which causes cell death, ~20 remain uncharacterized in this organism, whereas the others have been characterized experimentally and/or have had functions inferred based on sequence homology (Pombase, 12/09/2020, <https://www.pombase.org/>). Seven of these uncharacterized genes are evolutionarily conserved from yeasts to mammals, and here they are designated as conserved essential obscure (*ceo*) genes. According to their positions in the fission yeast genome, *ceo* genes were systematically numbered from *ceo1⁺* to *ceo7⁺* (Table 1). Three of the seven *ceo* genes (*ceo2⁺*, *ceo5⁺* and *ceo7⁺*) are essential, even in human cell lines (Blomen et al., 2015; Wang et al., 2015), and another (*ceo6⁺*) has been predicted as an essential human gene (Georgi et al., 2013). Human homologs of the five *ceo* genes (*ceo1⁺*, *ceo2⁺*, *ceo3⁺*, *ceo6⁺* and *ceo7⁺*) are thought to be involved in diseases when they malfunction (Belyaeva and Kedishvili, 2002; Blomen et al., 2015; Curbo et al., 2006; Fatima et al., 2021; Guimier et al., 2016; Matsuura et al., 2000; Pastore et al., 2021; Wang et al., 2009, 2015; Wilcox et al., 2007) (Table S1). Thus, revealing the functions of these genes might not only uncover unidentified physiological processes essential for cell viability, but might help to improve human health. Given that conditional mutants of these *ceo* genes have not been isolated to date, we studied their physiological roles using CRISPRi techniques.

First, *ceo* genes were knocked down using conventional CRISPRi with dCas9 and a single sgRNA. According to a previous report (Ishikawa et al., 2021), sgRNAs were designed to bind close to the TSS of the target *ceo* gene or ~90 bp downstream of the TSS (Fig. 3A–C). Fission yeast cells harboring a pSPdCas9-derived plasmid with one of the designed sgRNAs were cultivated in the presence of 20 μ M thiamine, which represses expression of dCas9 from the *nmt1-41* promoter, and then placed in medium without thiamine to induce dCas9 expression. As all *ceo* genes are essential for cell viability, knockdown of their expression was expected to inhibit colony formation. Consistent with this prediction, colony formation was clearly inhibited in *ceo3⁺* and *ceo5⁺* knockdown strains with two and three designed sgRNAs, respectively (Fig. 3D,E). Colony formation of a *ceo7⁺* gene knockdown strain was slightly inhibited (Fig. 3F). These observations demonstrate that dCas9-mediated CRISPRi is applicable for conditional knockdown of these *ceo* genes.

mRNA levels of *ceo* genes were examined in these CRISPRi knockdown strains. Cells were cultivated in the absence of thiamine for 26 h and mRNA levels were quantified by RT-qPCR (Fig. 3A–C). Consistent with inhibition of colony formation, the abundance of *ceo3⁺* mRNA was reduced by half (50–54%) in *ceo3⁺* knockdown cells harboring *ceo3-1* or *ceo3-2* sgRNA (Fig. 3A,D). Likewise, *ceo5-1*, *ceo5-2* and *ceo5-4* sgRNAs greatly reduced the level of *ceo5⁺* mRNA to 29–36% of the control, and *ceo7-7* sgRNA reduced *ceo7⁺* mRNA abundance to 54% of the control

Table 1. Summary of *ceo* genes knocked down by using CRISPRi

Gene name/synonym	Systematic ID	Product description	Human ortholog*	Transcriptional repression (%)	Method	Growth inhibition	Sufficient transcription index (%)	Cell morphology
<i>ceo1</i>	SPAC56F8.07	ER membrane integral protein	TMEM97	94.3	Double, dCas9	–	<5.7	–
<i>ceo2</i>	SPAC3A12.02	mitochondrial inorganic diphosphatase (predicted)	PPA1, PPA2	55.2	Double, dCas9	–	<44.8	–
<i>ceo3/pbr1</i>	SPAC19A8.06	ER oxidoreductase Pbr1	RDH14	53.7	Single, dCas9	+++	54.7	Plasmolysis
<i>ceo4/aim29</i>	SPAC2C4.04c	human C2orf76 ortholog	C2orf76	75.1	Double, dSpG	–	<24.9	–
<i>ceo5</i>	SPAC19B12.01	TPR repeat protein	TTC27	71.2	Single, dCas9	+	41.8	Elongation
<i>ceo6</i>	SPCC16C4.02c	Armadillo-type fold protein	NCDN	53.5	Double, dCas9	+	48.8	Elongation
<i>ceo7/mug160</i>	SPCC584.14	Armadillo repeat protein	ATXN10	48.6	Single, dCas9	+	55.8	–

*As from pombase (<https://www.pombase.org/>). Quantitative results are mean from three biological repeats. For growth inhibition: –, no growth inhibition; +, moderate growth inhibition; +++, strong growth inhibition. For cell morphology: –, normal morphology.

(Fig. 3B,C,E,F). Intriguingly, mRNA abundance and cell viability did not appear to correlate linearly. For example, *ceo3*⁺ mRNA levels were reduced to a similar extent by *ceo3*-1, *ceo3*-2 and *ceo3*-5 sgRNAs, but the extent of inhibition of colony formation by these sgRNAs differed greatly (Fig. 3A,D). *ceo3*-1 and *ceo3*-2 sgRNAs blocked colony formation nearly completely, whereas *ceo3*-5 did not. Similarly, *ceo5*-1, *ceo5*-2 and *ceo5*-4 sgRNAs inhibited colony formation, but *ceo5*-3 did not, although these four sgRNAs repressed transcription of the *ceo5*⁺ gene to a similar extent (Fig. 3B,E). These observations suggest that each gene might have a threshold value for reduction of the mRNA level, below which cell proliferation abruptly diminishes.

Expression of *ceo1*⁺ and *ceo6*⁺ genes was repressed efficiently by double sgRNA repression CRISPRi

As described above, conventional dCas9-mediated CRISPRi using one sgRNA was efficient enough to reduce colony formation when employed to knockdown *ceo3*⁺, *ceo5*⁺ and *ceo7*⁺ gene expression. However, this method did not inhibit colony formation when applied to *ceo1*⁺, *ceo2*⁺, *ceo4*⁺ and *ceo6*⁺ (Figs 4, 5; Fig. S2). These results suggest that efficiency of transcriptional repression by the conventional method was not sufficient to impair colony formation. To enhance transcriptional repression, we next utilized double sgRNA repression CRISPRi to knockdown expression of these genes, and expression of *ceo1*⁺ and *ceo6*⁺ was successfully repressed by combined use of two sgRNAs (Fig. 4). Four sgRNAs were designed for repression of *ceo6*⁺ expression. *ceo6*-1 binds to the non-template strand at the TSS, whereas *ceo6*-5, *ceo6*-6 and *ceo6*-3 bind to the template strand ~90 bp from the TSS (Fig. 4A). Although both *ceo6*-1 and *ceo6*-3 sgRNA alone could reduce the *ceo6*⁺ mRNA level by ~50%, neither could inhibit colony formation (Fig. 4A,C). When these two sgRNAs were applied in combination, the *ceo6*⁺ mRNA level decreased further and colony formation was inhibited (Fig. 4A,C). To repress *ceo1*⁺ gene expression, four sgRNAs, *ceo1*-9, *ceo1*-10, *ceo1*-11 and *ceo1*-12, were designed as illustrated in Fig. 4B. Although each of these sgRNAs individually could reduce the *ceo1*⁺ mRNA level to ~14% of that in the control with a nonsense sgRNA, combination of *ceo1*-9 and *ceo1*-11 further reduced the level to 4.8%. Given that a single vegetative cell normally contains 0.81 molecules of *ceo1*⁺ mRNA

(Marguerat et al., 2012), the result indicated that double repression with *ceo1*-9 and *ceo1*-11 sgRNAs reduced the *ceo1*⁺ mRNA abundance to ~0.04 molecule per cell, although colony formation was apparently not inhibited (Fig. 4D). The threshold *ceo1*⁺ mRNA level for cell proliferation is thus extremely low.

Knocking down *ceo4*⁺ transcription by dSpG-mediated CRISPRi

dSpG-mediated CRISPRi was applied to knockdown *ceo4*⁺ expression, as sgRNAs for dCas9 could not be designed at exactly the preferred spots due to the limitation of the PAM sequence (Fig. 5A). Together with three sgRNAs for dCas9, *ceo4*-5, *ceo4*-6 and *ceo4*-7, three more sgRNAs for dSpG, *ceo4*-8, *ceo4*-9 and *ceo4*-10, which bind closer to the preferred spots than those for dCas9 do, were examined for transcriptional repression. Five of the seven sgRNAs tested here reduced the *ceo4*⁺ mRNA level by ~70%. Double sgRNA repression by combining *ceo4*-9 and *ceo4*-10 sgRNAs further reduced the mRNA level to 21.5% of the control, which corresponds to ~0.67 molecule per cell (Marguerat et al., 2012) (Fig. 5A), although it apparently did not affect colony formation (Fig. 5B). As with *ceo1*⁺, the threshold of the *ceo4*⁺ mRNA level for cell proliferation is low.

The *ceo2*⁺ gene is resistant to CRISPRi targeting of preferred spots

The *ceo2*⁺ gene has at least five TSSs in a 25-bp region of its 5'UTR (Meylan et al., 2020), which makes it difficult to design sgRNAs that bind at the TSS or to ~90 bp downstream of the TSS. As attempts to repress *ceo2*⁺ transcription with dCas9- or SpG-mediated CRISPRi with a sgRNA that binds near these preferred spots (*ceo2*-3, *ceo2*-4 and *ceo2*-10) were unsuccessful, we sought for effective sgRNAs outside these spots (Fig. S2). Among those tested, three sgRNAs for dCas9 (*ceo2*-1, *ceo2*-12 and *ceo2*-13) reduced the *ceo2*⁺ mRNA level by 30–40% (Fig. S2B). Double sgRNA repression using a combination of *ceo2*-1 and *ceo2*-12 further reduced the mRNA level by 55%, although colony formation was not affected (Fig. S2B,C). Of note, the normal abundance of *ceo2*⁺ mRNA is estimated to be as low as 1.3 molecules in a single vegetative cell (~0.58/cell after CRISPRi) (Marguerat et al., 2012).

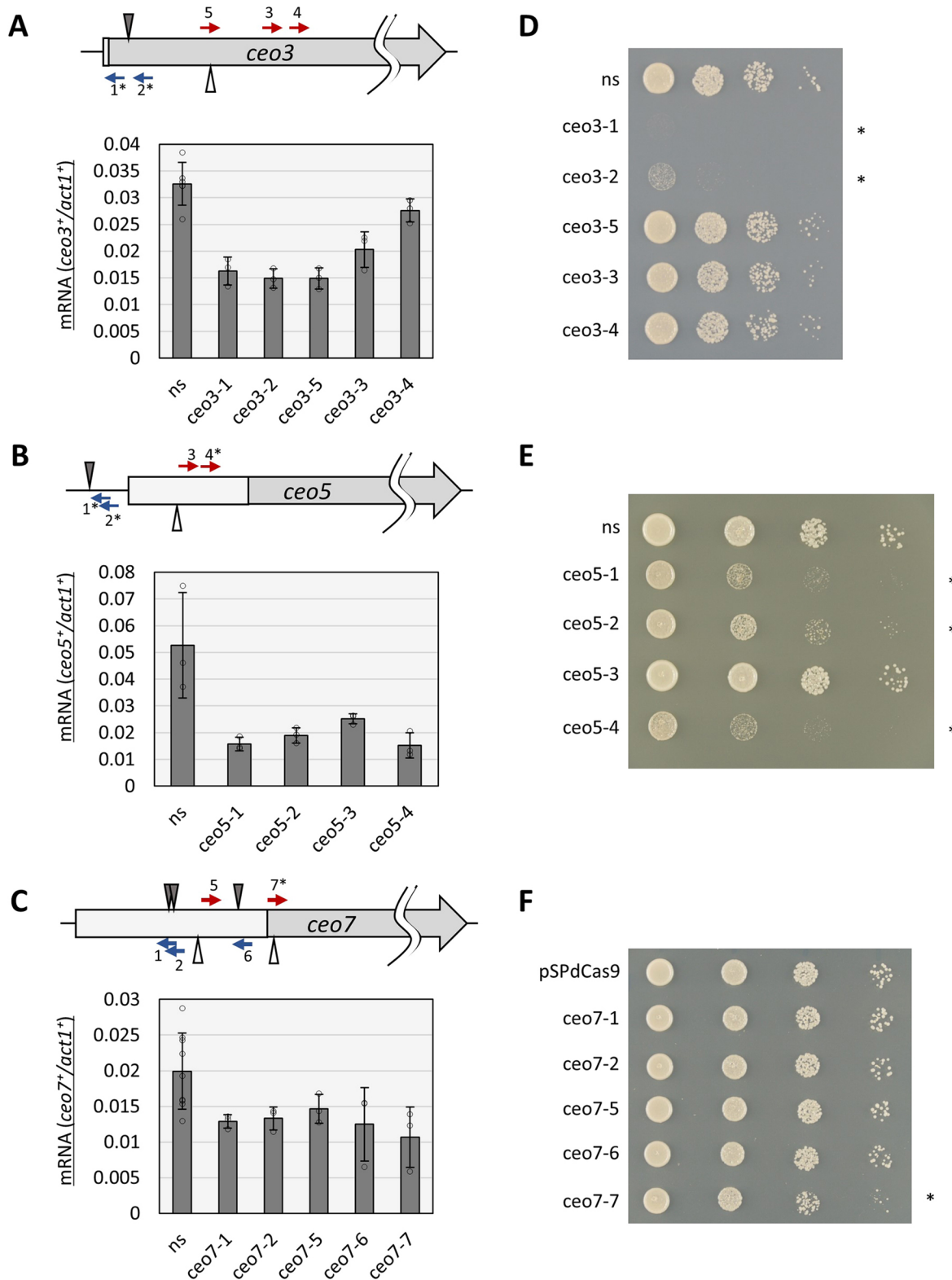


Fig. 3. Knockdown of *ceo3*⁺, *ceo5*⁺, and *ceo7*⁺ using conventional dCas9-mediated CRISPRi. (A–C) Top, targeting sequences designed for the indicated gene. Red and blue arrows indicate targeting sequences of sgRNAs that base-pair with the template and non-template strands of the targeted DNA, respectively. PAM sequences are situated at the immediate 3'-side of the arrowheads (not shown in the diagram). Gray triangle, TSS; white triangle, the position 90 bp downstream from the TSS; light gray box, 5'UTR; asterisks, targeting sequences that inhibited colony formation after induction of the CRISPRi. Bottom, quantification of mRNA. mRNA levels of the indicated gene and *act1*⁺ as determined by RT-qPCR. Relative mRNA amounts of target genes normalized by that of *act1*⁺ are presented. Data show means±s.d. from at least three biological replicates (ns in the panel A, *n*=6; ns in the panel C, *n*=9; others, *n*=3). ns, nonsense targeting sequence; open circle, individual data point. (D–F) Serial dilution (10-fold) spot test growth assays of fission yeast cells bearing CRISPRi plasmids with the indicated targeting sequences, on the EMM2 plate. Asterisks indicate inhibited colony formation. Images representative of two biological repeats.

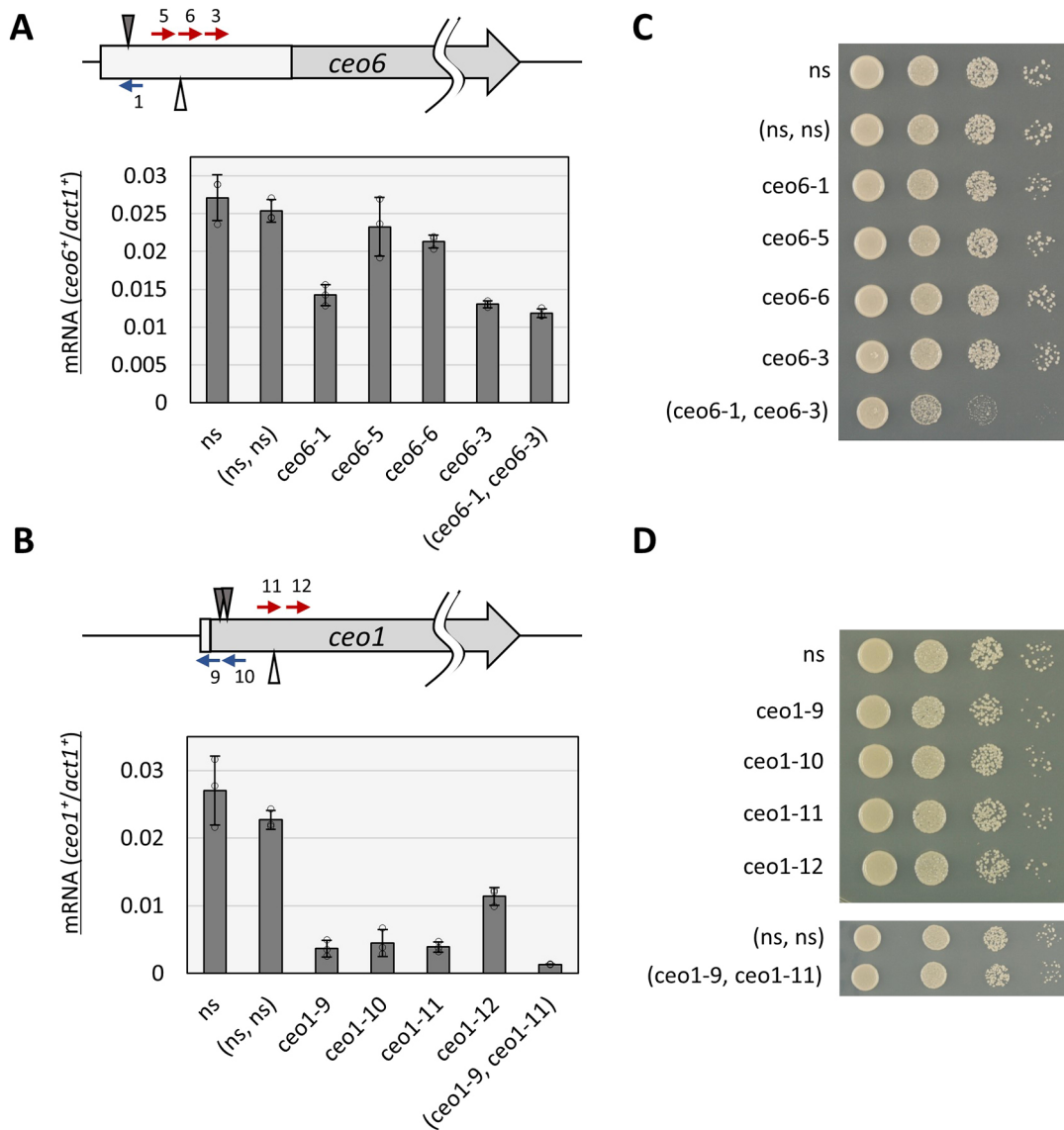


Fig. 4. Knockdown of *ceo6*⁺ and *ceo1*⁺ using dCas9-mediated double sgRNA repression. (A,B) Top, targeting sequences designed for the indicated gene. Red and blue arrows indicate targeting sequences of sgRNAs that base-pair with the template and non-template strands of the targeted DNA, respectively. PAM sequences are situated at the immediate 3'-side of the arrowheads (not shown in the diagram). Gray triangle, TSS; white triangle, the position 90 bp downstream from the TSS; light gray box, 5'UTR. Bottom, quantification of mRNA. mRNA levels of the indicated gene and *act1*⁺ were quantified by RT-qPCR. Relative mRNA amounts of target genes normalized by that of *act1*⁺ are presented. Data show means±s.d. from three biological replicates. ns, nonsense targeting sequence; open circle, individual data point. (C,D) Serial dilution (10-fold) spot test growth assays of fission yeast cells bearing CRISPRi plasmids with the indicated targeting sequences, on the EMM2 plate. Images representative of two biological repeats.

In summary, colony formation of strains knocked down on the *ceo1*⁺, *ceo2*⁺ or *ceo4*⁺ gene was indistinguishable from that of the nonsense control, although their transcription levels were reduced to less than one molecule per cell. It is possible that their mRNA and protein molecules have such long half-lives that a sufficient amount of protein was synthesized and accumulated from a small number of mRNA molecules; thus, their abundances were hardly reduced by CRISPRi repression.

Phenotypic analyses of *ceo* gene knockdown strains

As described above, we established *ceo* gene knockdown strains using CRISPRi. mRNA levels of targeted *ceo* genes in these strains decreased by 48.6% to 94.3% (Table 1). *ceo1*⁺, *ceo2*⁺ and *ceo6*⁺ gene expression was reduced most efficiently by double sgRNA repression dCas9-CRISPRi with combinations of ceo1-9

and ceo1-11, ceo2-1 and ceo2-12, and ceo6-1 and ceo6-3 sgRNAs, respectively. Gene expression of *ceo3*⁺, *ceo5*⁺ and *ceo7*⁺ was repressed most efficiently by conventional dCas9-CRISPRi using ceo3-2, ceo5-4 and ceo7-7 sgRNAs, respectively. *ceo4*⁺ gene expression was knocked down by the dSpG-mediated double sgRNA repression with ceo4-9 and ceo4-10 sgRNAs. Thus, knockdown strains with conventional or modified CRISPRi were used in the following experiments. Four out of the seven knockdown strains (*ceo3*⁺, *ceo5*⁺, *ceo6*⁺ and *ceo7*⁺) showed inhibited colony formation (Table 1, Fig. 6A,B; Fig. S3A). To prove that dCas9-mediated CRISPRi is applicable for characterizing physiological roles of essential genes, maximum growth rate (MGR, divisions/hour) in liquid culture and cellular morphology were analyzed in cells in which *ceo* gene expression was repressed.

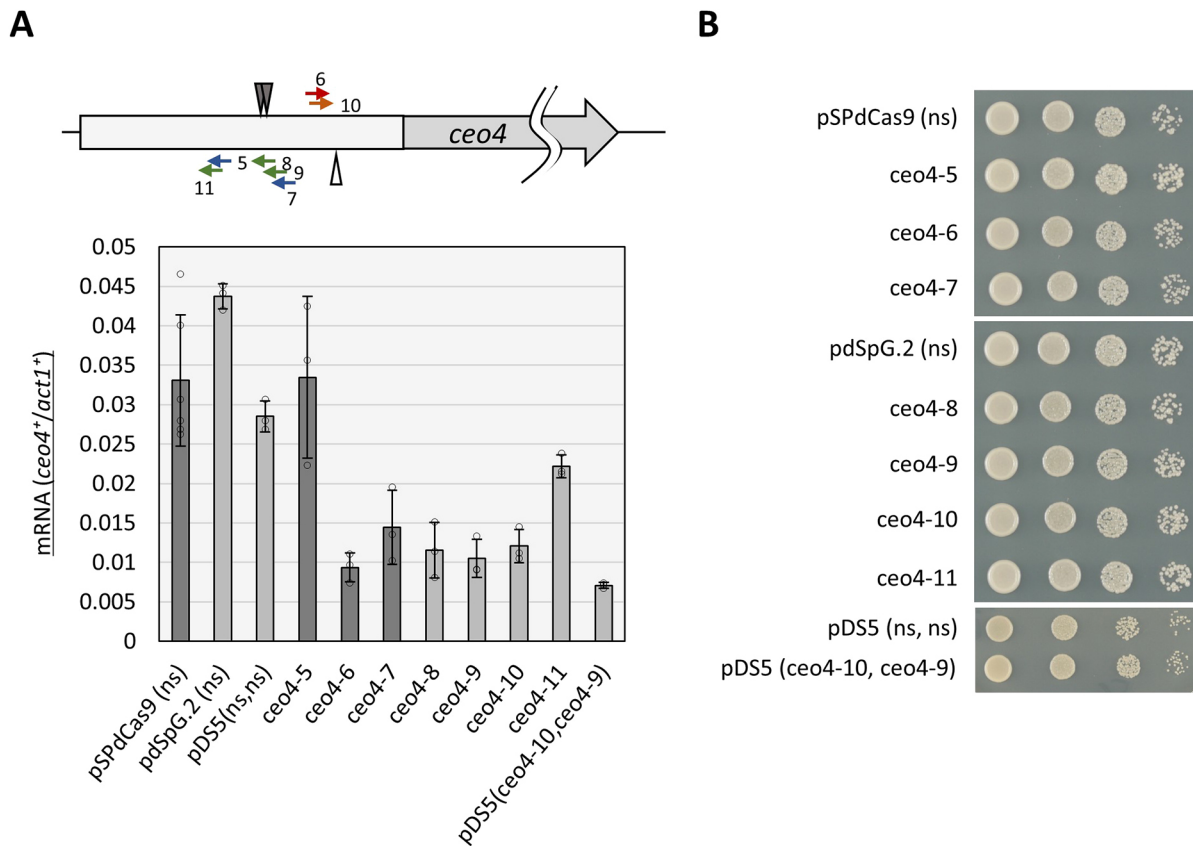


Fig. 5. Knockdown of *ceo4*⁺ using CRISPRi methods. (A) Top, targeting sequences designed for the *ceo4*⁺ gene. Red and blue arrows indicate targeting sequences of sgRNAs that base-pair with the template and non-template strands of the targeted DNA, respectively, for dCas9-mediated CRISPRi. Green and orange arrows indicate targeting sequences of sgRNAs that base-pair with the template and non-template strands of the targeted DNA, respectively, for the dSpG-mediated CRISPRi. PAM sequences are situated at the immediate 3'-side of the arrowheads (not shown in the diagram). Gray triangle, TSS; white triangle, the position 90 bp downstream from the TSS; light gray box, 5' UTR. Bottom, quantification of mRNA. mRNA levels of the indicated gene and *act1*⁺ were quantified by RT-qPCR. Relative mRNA amounts of target genes normalized by that of *act1*⁺ are presented. Dark gray bars indicate results of dCas9-mediated methods. Light bars indicate results of dSpG-mediated methods. Results show means ± s.d. from three biological replicates [pSPdCas9(ns), *n*=6; others, *n*=3]. ns, nonsense targeting sequence; open circle, individual data point. (B) Serial dilution (10-fold) spot test growth assays of fission yeast cells bearing CRISPRi plasmids with the indicated targeting sequences, on the EMM2 plate. Images representative of two biological repeats.

Inhibition of cell proliferation is reflected as a decrease of the MGR, which is the reciprocal of the minimum time required for cell density to double. The MGR was calculated by measuring the optical density at 600 nm (OD₆₀₀) of the cell culture as follows. After 50 h incubation in liquid Edinburgh minimal medium 2 (EMM2) without thiamine for induction of CRISPRi, *ceo* knockdown, cells were resuspended in fresh EMM2 and placed in a spectrometer equipped with a shaker and a heater. OD₆₀₀ of the cell culture was then measured every 30 min at 33°C (Fig. 6C,D, Fig. S3B). Growth rate (divisions/hour) was calculated every nine measurements (4 h). Among growth rates throughout an experiment, the maximum value was defined as the MGR (Fig. 6E, Fig. S3C; see Materials and Methods for details). MGRs of *ceo*-knockdown strains (*ceo*-KD strains) correlate with their colony formation ability on solid medium. For example, *ceo3*⁺ knockdown reduced MGR to 0.10 divisions/hour, whereas control cells grew at the MGR of 0.21 (Fig. 6E), consistent with severe growth retardation on solid medium by *ceo3*⁺ gene knockdown (Fig. 6A). Knockdown of *ceo7*⁺ gene expression, which resulted in only a slight decrease of colony formation on solid medium, apparently did not affect the MGR (Fig. 6A,E). It is of note that MGR might be overestimated because there can be an increase of OD caused by cellular elongation without cell division

observed in knockdown strains of *ceo5*⁺ and *ceo6*⁺ as described below.

To examine how *ceo* gene knockdown affects cell cycle progression and cell shape, *S. pombe* cells were fixed with glutaraldehyde before and after CRISPRi knockdown and stained with DAPI, which fluorescently labels nuclear DNA and surfaces of fixed fission yeast cells (Fig. 7). Control cells harboring a vector plasmid with nonsense sgRNA gene(s) showed normal cellular morphology before and after induction of dCas9 from the thiamine-repressive promoter. This indicates that expression of dCas9 and nonsense sgRNA does not affect cell shape or mitotic nuclear division (Fig. 7; Fig. S4). All *ceo* gene knockdown cells showed normal cell and nuclear morphology in the presence of thiamine, which represses expression of dCas9. After removal of thiamine for induction of dCas9, the *ceo5*⁺ and *ceo6*⁺ knockdown cells showed an elongated cell shape. As these elongated cells largely contain single nuclei, knockdown of the *ceo5*⁺ and *ceo6*⁺ genes might result in blocked or delayed cell cycle progression before mitotic nuclear division (Nurse et al., 1976). On the other hand, *ceo3*⁺ knockdown cells were short and slightly round, and they frequently showed plasmolysis-like morphology, in which cell surface materials strongly stained with DAPI accumulated and intruded into the cytoplasm. The *ceo3*⁺ gene product might be required for

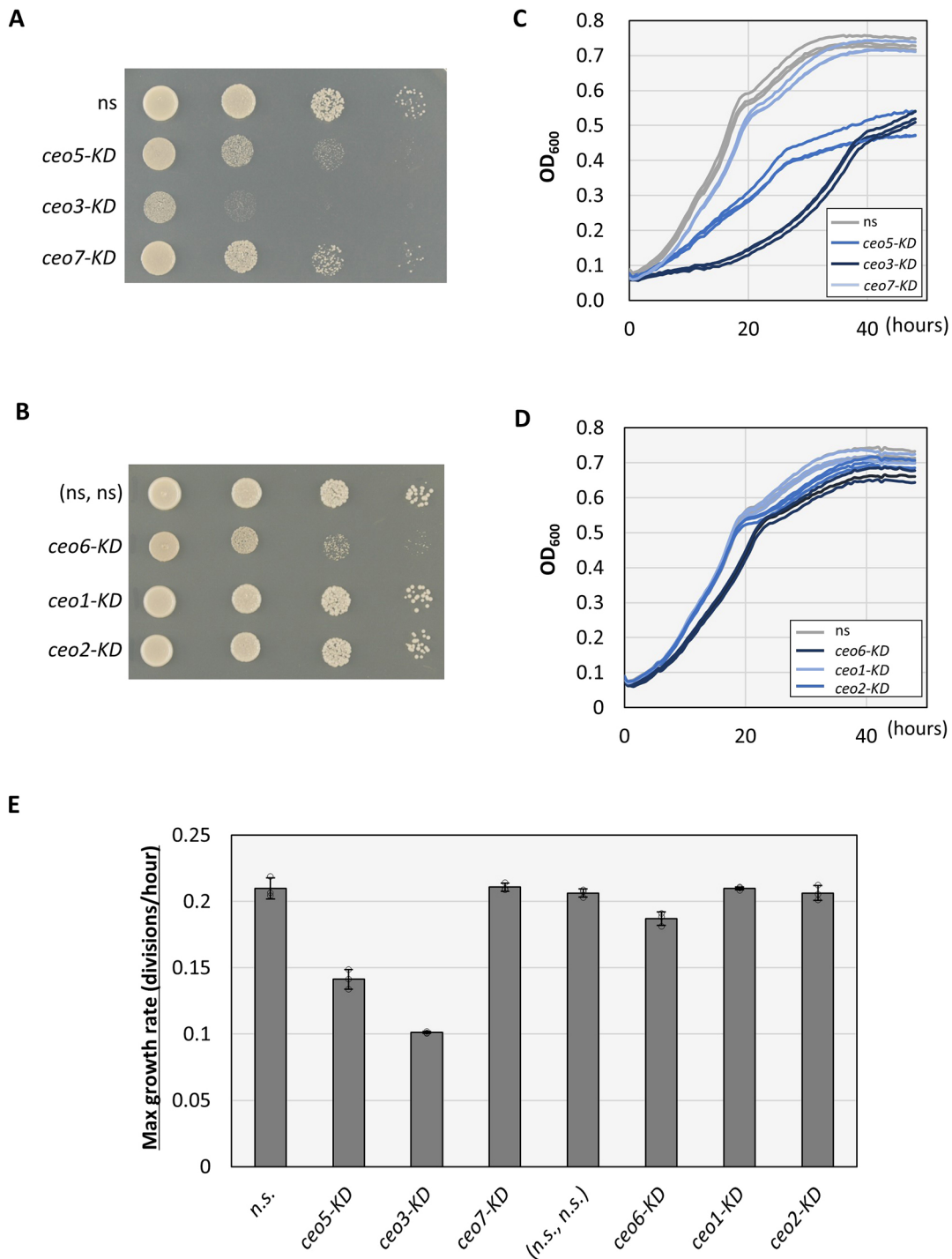


Fig. 6. Growth rate phenotypes of knockdown strains. (A,B) Serial dilution (10-fold) spot test growth assays of fission yeast cells bearing CRISPRi plasmids with the indicated targeting sequences, on the EMM2 plate. Images representative of three biological repeats. (C,D) Time course measurement of OD₆₀₀ after CRISPRi induction. Fission yeast cells carrying CRISPRi plasmids were grown in a microplate reader with OD₆₀₀ measurements at every 30 min after CRISPRi induction (see Materials and Methods for details). Results of three biological replicates are shown for each strain. (E) Maximum growth rate (divisions/hour) calculated from the results in C and D. Results show means±s.d. from three biological replicates. Open circles indicate individual data points.

maintenance of cell wall and/or cell membrane integrity. Collectively, CRISPRi enabled conditional knockdown of essential *ceo* genes and phenotypic analyses of knockdown cells. CRISPRi is a useful tool to characterize physiological roles of essential genes in *S. pombe* when their conditional lethal mutants are not available.

DISCUSSION

Analyzing the functions of essential genes in *S. pombe* has been challenging. This study showed that CRISPRi is a feasible option to resolve this issue by providing a systematic strategy to selectively knockdown expression of essential genes. Conventional dCas9-mediated CRISPRi successfully inhibited transcription of *ceo* genes

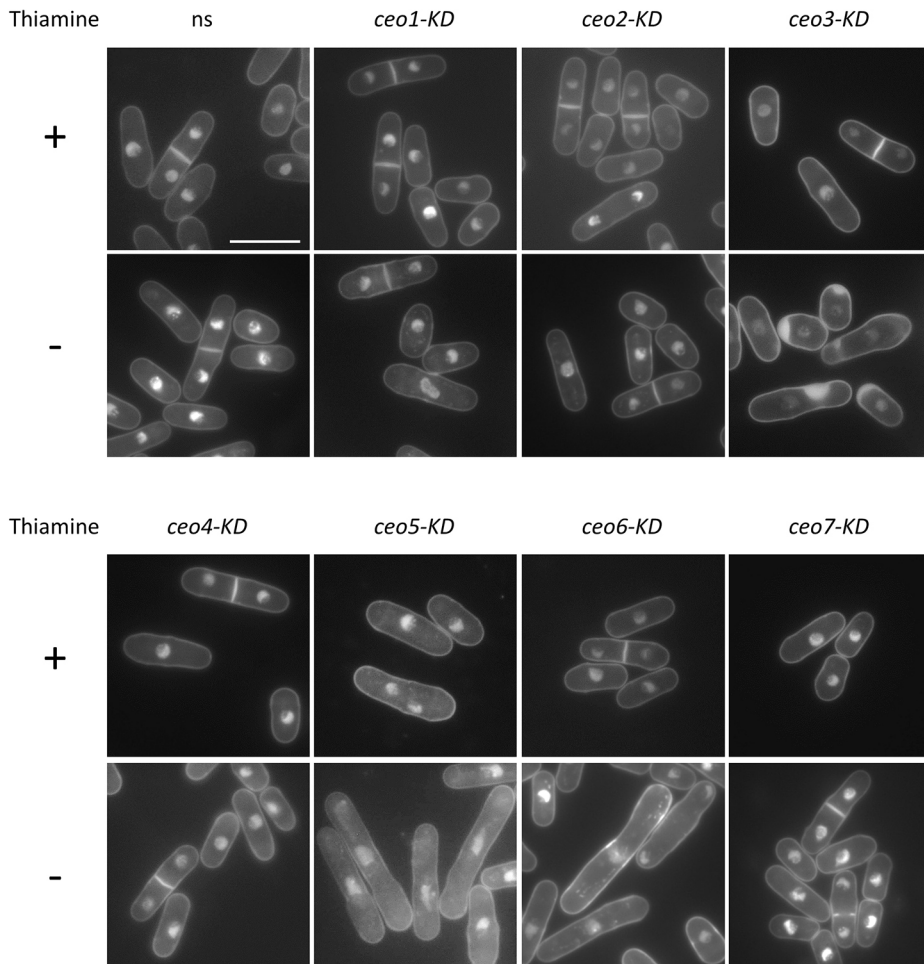


Fig. 7. Cell morphology phenotypes of knockdown strains. Fission yeast cells before (thiamine +) and after (thiamine –) 48 h of the CRISPRi induction were fixed with 2.5% glutaraldehyde and stained with DAPI, followed by fluorescence microscopy (see Materials and Methods for details). ns, fission yeast cells carrying the plasmid, pSPdCas9, which codes nonsense sgRNA; KD, knockdown strains. Scale bar: 10 μ m.

efficiently enough to inhibit cell proliferation of knockdown strains of *ceo3*⁺, *ceo5*⁺ and *ceo7*⁺. The double sgRNA repression technique implemented in this study enhances transcriptional repression efficiency, and successfully repressed *ceo6*⁺ gene expression to inhibit cell proliferation. dSpG-mediated CRISPRi is also useful, particularly in cases in which canonical PAM sequences of dCas9 (5'-NGG) are not available at preferred target gene sites. *ceo4*⁺ gene expression was reduced by 75% using dSpG in combination with the double sgRNA repression technique. To prove that CRISPRi is applicable for functional characterization of essential genes, physiological roles of *ceo* genes were analyzed by utilizing the gene knockdown strains constructed above – knockdown of *ceo5*⁺ and *ceo6*⁺ genes resulted in cell elongation, whereas *ceo3*⁺ knockdown caused cell shortening and a plasmolysis-like phenotype, implying that these *ceo* genes might be involved in cell cycle control and/or maintenance of cell shape integrity. Thus, CRISPRi provides an alternative means of characterizing function of essential genes in *S. pombe* when suitable conditional lethal mutant alleles are not available.

Based on our experience with systematic knockdown of *ceo* genes by CRISPRi in this study, we propose a protocol to construct CRISPRi knockdown strains as follows. (1) Test whether conventional dCas9-mediated CRISPRi with a single sgRNA, which preferably binds at the TSS or ~90 bp downstream of the TSS, can sufficiently repress expression of the target gene. (2) If expression of the target gene is not sufficiently repressed by conventional CRISPRi, the double sgRNA repression method

should be considered. (3) If the mRNA level of the target gene is not reduced even with double sgRNA method, dSpG-mediated CRISPRi should be employed with either a single or double sgRNAs.

During construction of *ceo* gene knockdown strains, we obtained a series of strains in which mRNA levels of the *ceo* genes decreased to various extents, and we found that subtle differences in the mRNA level often resulted in large differences in cell proliferation. Although we do not know whether this abrupt reduction of cell proliferation at a particular level of transcription holds true for all essential genes, it would be expected that there is a threshold mRNA level for each essential gene that is required to support normal cell proliferation. Knockdown strains constructed in this study allowed us to calculate such a threshold, designated as the 'sufficient transcription index' for *ceo* genes (Table 1). The sufficient transcription index was calculated as the average of the minimal transcription level that supported normal colony formation and the maximum transcription level that failed to support normal colony formation. Among *ceo* genes, the highest value of the sufficient transcription index was 55.8% (*ceo7*⁺), and this suggests that essential genes are often functional even when their transcription rate decreased to ~60% of normal. Therefore, when CRISPRi for an essential gene does not decrease the mRNA to less than 60%, it is worth seeking conditions that improve repression efficiency by using double sgRNA repression and/or dSpG, to develop a conditionally defective strain.

Among human homologs of the seven *ceo* genes, six genes are involved in cancer cell viability and/or human diseases (Table S1)

(Belyaeva and Kedishvili, 2002; Blomen et al., 2015; Curbo et al., 2006; Fatima et al., 2021; Georgi et al., 2013; Guimier et al., 2016; Matsuura et al., 2000; Pastore et al., 2021; Wang et al., 2009, 2015; Wilcox et al., 2007), implying that their essential roles are conserved evolutionarily from fission yeast to humans. Although the precise molecular functions of these gene products remain largely unknown, morphological defects caused by CRISPRi gene knockdown strongly suggest that *ceo5*⁺ and *ceo6*⁺ function in normal cell cycle progression, and that *ceo3*⁺ helps to maintain the integrity of cellular structures (Fig. 7). Interestingly, a high-throughput study showed that overproduced fluorescently labeled Ceo6 protein was localized at the spindle pole body in *S. pombe* (Matsuyama et al., 2006); thus, Ceo6 protein might contribute to formation of the mitotic spindle, which is essential for chromosome segregation. The same report found that Ceo3 protein was localized on the cell surface and as cytoplasmic dots, and this is consistent with our hypothesis that Ceo3 is involved in maintaining integrity of cell surface structure (Matsuyama et al., 2006). Detailed studies of Ceo proteins will help reveal how their human orthologs contribute to human health, and the CRISPRi strains constructed here are useful resources for such studies.

The present study shows that CRISPRi is a feasible option to characterize essential gene functions in *S. pombe*. Plasmid-based CRISPRi for fission yeast is easy to handle for knockdown of essential genes. This method is suitable for high-throughput applications such as construction of a genome-wide *S. pombe* gene knockdown strain library, which complements the haploid gene deletion strain library covering the only non-essential genes (Kim et al., 2010). Thus, CRISPRi in fission yeast will expand accessibility to genetic analyses for functional characterization of essential genes and greatly advance understanding of their conserved functions among eukaryotes.

MATERIALS AND METHODS

Media and fission yeast strains

Growth media and yeast culture conditions were as previously described (Moreno et al., 1991). Edinburgh Minimal Medium 2 (EMM2) contains 2% glucose. EMM2 supplemented with 20 μ M thiamine (EMM2+T20) was utilized to repress CRISPRi of fission yeast strains. A low-adenine medium to detect repressed *ade6*⁺ gene expression was prepared by supplementing EMM2 with 7.5 mg/l adenine. Fission yeast (*S. pombe*) strains carrying a plasmid for CRISPRi were prepared by transformation of strain sp685 (*h⁻leu1⁻*) using the standard lithium acetate method.

Plasmid constructions

The pSPdCas9.5 plasmid was constructed by modifying the pSPdCas9 plasmid, which contain a sgRNA gene and a *dCas9* gene (Ishikawa et al., 2021). To insert an additional sgRNA gene into pSPdCas9, a cloning site was inserted into it by ligating a double-stranded oligo-DNA containing restriction sites (PmeI and BamHI) at the plasmid SbfI site. The resulting plasmid with this additional cloning site was named pSPdCas9.2 (Fig. 1A). A PaqCI-site version of the sgRNA gene (sgRNA2) was constructed by inserting a double-stranded oligo-DNA containing two PaqCI sites into the BbsI-cleaved sgRNA gene on pSPdCas9. This plasmid (pSPdCas9.3) was utilized as a template to amplify a DNA fragment containing the sgRNA2 by polymerase chain reaction (PCR) with primers KI1169 and KI1248 (see Table S2 for primer sequences). The PCR product was cleaved with BamHI and was then ligated into the PmeI-BamHI site of the pSPdCas9.2. The resulting plasmid containing two sgRNA genes was named pSPdCas9.5 (Fig. 1B).

The SpG version of pSPdCas9.2, which was named pdSpG.2 (Fig. 1C), was constructed as follows. A 1553-bp DNA fragment, including SpG mutations that cause amino acid substitutions D1135L, S1136W, G1218K, E1219Q, R1335Q and T1337R, was amplified from plasmid

pCAG-CBE4max-SpG-P2A-EGFP (Addgene 139998) by PCR with primers KI1423 and KI1424 (Walton et al., 2020). This DNA fragment was integrated into the corresponding region of pSPdCas9.2 by recombination with another DNA fragment amplified from pSPdCas9.2 by PCR with KI1425 and KI1426 (Nozaki and Niki, 2019). Given that the latter fragment contains mutations that cause amino acid substitutions at catalytic residues (D10A and H840A), the SpG encoded in pdSpG.2 is catalytically inactive (we call this mutant protein dead SpG or dSpG). pdSpG.2 was further modified to construct another plasmid for dSpG-mediated, double sgRNA repression (pdSpG.5, Fig. 1D), by inserting the DNA fragment containing the sgRNA2 to the pdSpG.2 in the same way as for pSPdCas9.5 construction.

Modifications of targeting sequences of sgRNAs on plasmids used in this study were conducted as previously reported (Ishikawa et al., 2021). Genomic positions of TSSs utilized to design targeting sequences of sgRNAs were previously determined (Li et al., 2015; Meylan et al., 2020). 5' UTR regions indicated in this study were obtained from Pombase (<https://www.pombase.org/>). DNA sequences of targeting sequences and primers are available in Table S2. A plasmids list with brief descriptions on their structures is available in Table S3.

Induction of CRISPRi

dCas9-mediated CRISPRi used in this study is conditionally inducible (Ishikawa et al., 2021). Transcription of the *dCas9* gene is controlled by the *mtl-41p* promoter, which is fully inhibited in the presence of 15 μ M thiamine in media (Forsburg, 1993). Removing thiamine from the media induces dCas9 transcription and then CRISPRi. This procedure was conducted as previously reported (Ishikawa et al., 2021). Briefly, before induction of CRISPRi, fission yeast strains were grown on EMM2 plates supplemented with 20 μ M thiamine at 33°C for about 24 h. To induce CRISPRi, cells were extensively washed and were subjected to culture in EMM2 liquid medium without thiamine for 6 h. This culture was diluted to 9.4×10^4 cells/ml in EMM2 medium without thiamine, followed by incubation at 33°C for 20 h.

Cell growth evaluation

Inhibition of cellular growth by gene knockdown was estimated by two methods, colony formation and growth rate measurement. Colony formation was observed by spotting serial dilutions of cell culture on EMM2 plates after CRISPRi induction described above, followed by incubation at 33°C for 3 days. The maximum growth rate was measured as previously described, with some modifications (Makanee et al., 2013). A cell culture after CRISPRi induction was diluted two-fold with EMM2 and was cultured at 33°C for 24 h. To adjust cell density to levels suitable for optical density (OD) measurement, the resulting culture was diluted ten-fold with EMM2, and the diluted culture was further incubated at 33°C for 48 h, while monitoring the OD₆₀₀ every 30 min, using a microplate reader HiTS (SCINICS Co., Ltd., Tokyo, Japan). Growth rate (cell divisions/hour) was calculated as the slope of the line best fit to every nine data points of log₂(OD₆₀₀) versus time (hour), using the least squares method. Maximum growth rate (divisions/hour) is the highest growth rate during the 48 h. The reciprocal of the maximum growth rate indicates minimum doubling time (h).

RT-qPCR

Transcription of target genes was quantified using reverse transcription quantitative PCR (RT-qPCR), as previously reported (Lyne et al., 2003). In brief, after CRISPRi induction, cells were washed with sterilized water and stored at -80°C until total RNA preparation. Total RNA was prepared by acid phenol-chloroform extraction. cDNA was prepared using a ReverTra Ace qPCR RT kit according to manufacturer instructions (TOYOBO Co., Ltd., Tsuruga, Japan). cDNAs were quantified with a real-time PCR instrument (LightCycler, Roche, Ltd., Basel, Switzerland) and FastStart Essential DNA Green Master Mix (Roche, Ltd., Basel, Switzerland), under standard reaction conditions (pre-incubation at 95°C for 10 min, then 45 cycles of 95°C for 10 s, 60°C for 10 s, and 72°C for 10 s, followed by melting from 65°C to 97°C). Amplification of a single PCR product with

each primer set was confirmed by melt curve analysis. mRNA levels of target genes were quantified as values relative to that of *act1⁺*. Data show the mean \pm s.d. from at least three biological replicates. Each value of the biological replicates was calculated as the mean of three technical replicates of qPCR measurements. One data point of pSPdCas9 (ns) was excluded from a data analysis shown in the Fig. S2B as an outlier (its value is higher than the mean by two-fold of the standard deviation). All the other data points were included in data analyses. DNA sequences of qPCR primers are shown in Table S2.

Cell morphological analysis

Liquid EMM2+T20 medium (2 ml) was inoculated with a single colony grown on an EMM2+T20 plate and incubated at 33°C for 24 h with shaking. This culture was diluted with 10 ml of EMM2+T20 and was grown to log-phase. An aliquot of this log-culture before CRISPRi induction was recovered and fixed for cell morphology analysis. In order to remove thiamine, the other part of the log-culture was washed six times with 1 ml of sterilized water and then resuspended in 1 ml of water. Washed cells were diluted and grown 48 h in EMM2 medium at 33°C with shaking. During this incubation, the cell culture was diluted twice so as not to reach stationary phase. Cells before and after CRISPRi induction were fixed with 2.5% of glutaraldehyde on ice for 30 min. Fixed cells were washed twice with phosphate-buffered saline (PBS) and subjected to fluorescence microscopy in presence of 25 μ g/ml DAPI using a fluorescence microscope (EVOS, Thermo Fisher Scientific Inc., Waltham, USA).

Reagent availability

Plasmids pSPdCas9, pSPdCas9.2, pSPdCas9.3, pSPdCas9.5, pdSpG.2, pDS_{sa2}, and pdSpG.5 will be available at National BioResource Project (<https://yeast.nig.ac.jp/yeast/top.xhtml>). Other strains and plasmids are available upon request.

Acknowledgements

We thank our colleagues Dr Yusuke Toyoda, Fumie Masuda, Yuri Okabe and Hidefumi Tokunou for valuable discussions.

Competing interests

The authors declare no competing or financial interests.

Author contributions

Conceptualization: K.I., S. Saitoh; Methodology: K.I., S. Saitoh; Validation: K.I., S. Saitoh; Formal analysis: K.I., S. Soejima; Investigation: K.I., S. Soejima, S. Saitoh; Resources: K.I., S. Soejima; Data curation: K.I.; Writing - original draft: K.I., S. Saitoh; Writing - review & editing: K.I., S. Saitoh; Visualization: K.I.; Supervision: K.I., S. Saitoh; Project administration: K.I., S. Saitoh; Funding acquisition: K.I., S. Saitoh.

Funding

This study was partially supported by grants from the Kurume University Millennium Box Foundation for the Promotion of Science, the Ishibashi Foundation for the Promotion of Science, the Kakihara Foundation for Science and Technology to K.I., the Fukuoka Bio-valley Project to K.I. and S. Saitoh, Grants-in-Aid for Scientific Research (C) from the Japan Society for the Promotion of Science (17K07394 and 20K06648 to S. Saitoh), and by the MEXT-supported program for the strategic research foundation at private universities from the Ministry of Education, Culture, Sports, Science and Technology, Japan.

Data availability

All relevant data can be found within the article and its supplementary information.

References

Bähler, J., Wu, J.-Q., Longtine, M. S., Shah, N. G., McKenzie, A., III, Steever, A. B., Wach, A., Philippsen, P. and Pringle, J. R. (1998). Heterologous modules for efficient and versatile PCR-based gene targeting in *Schizosaccharomyces pombe*. *Yeast* **14**, 943-951. doi:10.1002/(SICI)1097-0061(199807)14:10<943::AID-YEA292>3.0.CO;2-Y

Belyaeva, O. V. and Kedishvili, N. Y. (2002). Human pancreas protein 2 (PAN2) has a retinal reductase activity and is ubiquitously expressed in human tissues. *FEBS Lett.* **531**, 489-493. doi:10.1016/S0014-5793(02)03588-3

Bikard, D., Jiang, W., Samai, P., Hochschild, A., Zhang, F. and Marraffini, L. A. (2013). Programmable repression and activation of bacterial gene expression

using an engineered CRISPR-Cas system. *Nucleic Acids Res.* **41**, 7429-7437. doi:10.1093/nar/gkt520

Blomen, V. A., Májek, P., Jae, L. T., Bigenzahn, J. W., Nieuwenhuis, J., Staring, J., Sacco, R., van Diemen, F. R., Oik, N., Stukalov, A. et al. (2015). Gene essentiality and synthetic lethality in haploid human cells. *Science* **350**, 1092-1096. doi:10.1126/science.aac7557

Curbo, S., Lagier-Tourenne, C., Carozzo, R., Palenzuela, L., Lucio, S., Hirano, M., Santorelli, F., Arenas, J., Karlsson, A. and Johansson, M. (2006). Human mitochondrial pyrophosphatase: cDNA cloning and analysis of the gene in patients with mtDNA depletion syndromes. *Genomics* **87**, 410-416. doi:10.1016/j.ygeno.2005.09.017

Fatima, A., Hoerber, J., Schuster, J., Koshimizu, E., Maya-Gonzalez, C., Keren, B., Mignot, C., Akram, T., Ali, Z., Miyatake, S. et al. (2021). Monoallelic and bi-allelic variants in NCDN cause neurodevelopmental delay, intellectual disability, and epilepsy. *Am. J. Hum. Genet.* **108**, 739-748. doi:10.1016/j.ajhg.2021.02.015

Forsburg, S. L. (1993). Comparison of *Schizosaccharomyces pombe* expression systems. *Nucleic Acids Res.* **21**, 2955-2956. doi:10.1093/nar/21.12.2955

Georgi, B., Voight, B. F. and Bućan, M. (2013). From mouse to human: evolutionary genomics analysis of human orthologs of essential genes. *PLoS Genet.* **9**, e1003484. doi:10.1371/journal.pgen.1003484

Gilbert, L. A., Horlbeck, M. A., Adamson, B., Villalta, J. E., Chen, Y., Whitehead, E. H., Guimaraes, C., Panning, B., Ploegh, H. L., Bassik, M. C. et al. (2014). Genome-scale CRISPR-mediated control of gene repression and activation. *Cell* **159**, 647-661. doi:10.1016/j.cell.2014.09.029

Guimier, A., Gordon, C. T., Godard, F., Ravenscroft, G., Oufadem, M., Vasnier, C., Rambaud, C., Nitschke, P., Bole-Feysot, C., Masson, C. et al. (2016). Biallelic PPA2 mutations cause sudden unexpected cardiac arrest in infancy. *Am. J. Hum. Genet.* **99**, 666-673. doi:10.1016/j.ajhg.2016.06.021

Hayashi, A. and Tanaka, K. (2019). Short-Homology-Mediated CRISPR/Cas9-Based Method for Genome Editing in Fission Yeast. *G3 (Bethesda)* **9**, 1153-1163. doi:10.1534/g3.118.200976

Ishikawa, K., Soejima, S., Masuda, F. and Saitoh, S. (2021). Implementation of dCas9-mediated CRISPRi in the fission yeast *Schizosaccharomyces pombe*. *G3 (Bethesda)* **11**, jkab051. doi:10.1093/g3journal/jkab051

Jacobs, J. Z., Ciccaglione, K. M., Tournier, V. and Zaratiegui, M. (2014). Implementation of the CRISPR-Cas9 system in fission yeast. *Nat. Commun.* **5**, 5344. doi:10.1038/ncomms6344

Jinek, M., Chylinski, K., Fonfara, I., Hauer, M., Doudna, J. A. and Charpentier, E. (2012). A programmable dual-RNA-guided DNA endonuclease in adaptive bacterial immunity. *Science* **337**, 816-821. doi:10.1126/science.1225829

Kanke, M., Nishimura, K., Kanemaki, M., Kakimoto, T., Takahashi, T. S., Nakagawa, T. and Masukata, H. (2011). Auxin-inducible protein depletion system in fission yeast. *BMC Cell Biol.* **12**, 8. doi:10.1186/1471-2121-12-8

Kim, D.-U., Hayles, J., Kim, D., Wood, V., Park, H.-O., Won, M., Yoo, H.-S., Duhig, T., Nam, M., Palmer, G. et al. (2010). Analysis of a genome-wide set of gene deletions in the fission yeast *Schizosaccharomyces pombe*. *Nat. Biotechnol.* **28**, 617-623. doi:10.1038/nbt.1628

Knott, G. J. and Doudna, J. A. (2018). CRISPR-Cas guides the future of genetic engineering. *Science* **361**, 866-869. doi:10.1126/science.aat5011

Lawhorn, I. E. B., Ferreira, J. P. and Wang, C. L. (2014). Evaluation of sgRNA target sites for CRISPR-mediated repression of TP53. *PLoS ONE* **9**, e113232. doi:10.1371/journal.pone.0113232

Li, H., Hou, J., Bai, L., Hu, C., Tong, P., Kang, Y., Zhao, X. and Shao, Z. (2015). Genome-wide analysis of core promoter structures in *Schizosaccharomyces pombe* with DeepCAGE. *RNA Biol.* **12**, 525-537. doi:10.1080/15476286.2015.1022704

Lyne, R., Burns, G., Mata, J., Penkett, C. J., Rustici, G., Chen, D., Langford, C., Vetrie, D. and Bähler, J. (2003). Whole-genome microarrays of fission yeast: characteristics, accuracy, reproducibility, and processing of array data. *BMC Genomics* **4**, 27. doi:10.1186/1471-2164-4-27

Makanae, K., Kintaka, R., Makino, T., Kitano, H. and Moriya, H. (2013). Identification of dosage-sensitive genes in *Saccharomyces cerevisiae* using the genetic tug-of-war method. *Genome Res.* **23**, 300-311. doi:10.1101/gr.146662.112

Marguerat, S., Schmidt, A., Codlin, S., Chen, W., Aebersold, R. and Bähler, J. (2012). Quantitative analysis of fission yeast transcriptomes and proteomes in proliferating and quiescent cells. *Cell* **151**, 671-683. doi:10.1016/j.cell.2012.09.019

Matsuura, T., Yamagata, T., Burgess, D. L., Rasmussen, A., Grewal, R. P., Watake, K., Khajavi, M., McCall, A. E., Davis, C. F., Zu, L. et al. (2000). Large expansion of the ATTCT pentanucleotide repeat in spinocerebellar ataxia type 10. *Nat. Genet.* **26**, 191-194. doi:10.1038/79911

Matsuyama, A., Arai, R., Yashiroda, Y., Shirai, A., Kamata, A., Sekido, S., Kobayashi, Y., Hashimoto, A., Hamamoto, M., Hiraoka, Y. et al. (2006). ORFome cloning and global analysis of protein localization in the fission yeast *Schizosaccharomyces pombe*. *Nat. Biotechnol.* **24**, 841-847. doi:10.1038/nbt1222

McGlincy, N. J., Meacham, Z. A., Reynaud, K. K., Muller, R., Baum, R. and Ingolia, N. T. (2021). A genome-scale CRISPR interference guide library enables comprehensive phenotypic profiling in yeast. *BMC Genomics* **22**, 205. doi:10.1186/s12864-021-07518-0

- Meylan, P., Dreos, R., Ambrosini, G., Groux, R. and Bucher, P. (2020). EPD in 2020: enhanced data visualization and extension to ncRNA promoters. *Nucleic Acids Res.* **48**, D65-D69. doi:10.1093/nar/gkz1014
- Moreno, S., Klar, A. and Nurse, P. (1991). Molecular genetic analysis of fission yeast *Schizosaccharomyces pombe*. *Methods Enzymol.* **194**, 795-823. doi:10.1016/0076-6879(91)94059-L
- Nozaki, S. and Niki, H. (2019). Exonuclease III (XthA) enforces in vivo DNA cloning of *Escherichia coli* to create cohesive ends. *J. Bacteriol.* **201**, e00660-18. doi:10.1128/JB.00660-18
- Nurse, P., Thuriaux, P. and Nasmyth, K. (1976). Genetic control of the cell division cycle in the fission yeast *Schizosaccharomyces pombe*. *Mol. Gen. Genet.* **146**, 167-178. doi:10.1007/BF00268085
- Pastore, S. F., Muhammad, T., Harripaul, R., Lau, R., Khan, M. T. M., Khan, M. I., Islam, O., Kang, C., Ayub, M., Jelani, M. et al. (2021). Biallelic inheritance in a single Pakistani family with intellectual disability implicates new candidate gene RDH14. *Sci. Rep.* **11**, 23113. doi:10.1038/s41598-021-02599-z
- Qi, L. S., Larson, M. H., Gilbert, L. A., Doudna, J. A., Weissman, J. S., Arkin, A. P. and Lim, W. A. (2013). Repurposing CRISPR as an RNA-guided platform for sequence-specific control of gene expression. *Cell* **152**, 1173-1183. doi:10.1016/j.cell.2013.02.022
- Rodríguez-López, M., Cotobal, C., Fernández-Sánchez, O., Borbarán Bravo, N., Oktriani, R., Abendroth, H., Uka, D., Hoti, M., Wang, J., Zariatigui, M. et al. (2016). A CRISPR/Cas9-based method and primer design tool for seamless genome editing in fission yeast. *Wellcome Open Res.* **1**, 19. doi:10.12688/wellcomeopenres.10038.1
- Roguev, A., Bandyopadhyay, S., Zofall, M., Zhang, K., Fischer, T., Collins, S. R., Qu, H., Shales, M., Park, H.-O., Hayles, J. et al. (2008). Conservation and rewiring of functional modules revealed by an epistasis map in fission yeast. *Science* **322**, 405-410. doi:10.1126/science.1162609
- Schuldiner, M., Collins, S. R., Thompson, N. J., Denic, V., Bhamidipati, A., Punna, T., Ihmels, J., Andrews, B., Boone, C., Greenblatt, J. F. et al. (2005). Exploration of the function and organization of the yeast early secretory pathway through an epistatic miniarray profile. *Cell* **123**, 507-519. doi:10.1016/j.cell.2005.08.031
- Sternberg, S. H., Redding, S., Jinek, M., Greene, E. C. and Doudna, J. A. (2014). DNA interrogation by the CRISPR RNA-guided endonuclease Cas9. *Nature* **507**, 62-67. doi:10.1038/nature13011
- Walton, R. T., Christie, K. A., Whittaker, M. N. and Kleinstiver, B. P. (2020). Unconstrained genome targeting with near-PAMless engineered CRISPR-Cas9 variants. *Science* **368**, 290-296. doi:10.1126/science.aba8853
- Wang, H., Westin, L., Nong, Y., Birnbaum, S., Bendor, J., Brismar, H., Nestler, E., Aperia, A., Flajolet, M. and Greengard, P. (2009). Norbin is an endogenous regulator of metabotropic glutamate receptor 5 signaling. *Science* **326**, 1554-1557. doi:10.1126/science.1178496
- Wang, T., Birsoy, K., Hughes, N. W., Krupczak, K. M., Post, Y., Wei, J. J., Lander, E. S. and Sabatini, D. M. (2015). Identification and characterization of essential genes in the human genome. *Science* **350**, 1096-1101. doi:10.1126/science.aac7041
- Wilcox, C. B., Feddes, G. O., Willett-Brozick, J. E., Hsu, L.-C., DeLoia, J. A. and Baysal, B. E. (2007). Coordinate up-regulation of TMEM97 and cholesterol biosynthesis genes in normal ovarian surface epithelial cells treated with progesterone: implications for pathogenesis of ovarian cancer. *BMC Cancer* **7**, 223. doi:10.1186/1471-2407-7-223
- Zhang, X.-R., He, J.-B., Wang, Y.-Z. and Du, L.-L. (2018). A cloning-free method for CRISPR/Cas9-mediated genome editing in fission yeast. *G3 (Bethesda)* **8**, 2067-2077. doi:10.1534/g3.118.200164
- Zhao, Y. and Boeke, J. D. (2020). CRISPR-Cas12a system in fission yeast for multiplex genomic editing and CRISPR interference. *Nucleic Acids Res.* **48**, 5788-5798. doi:10.1093/nar/gkaa329

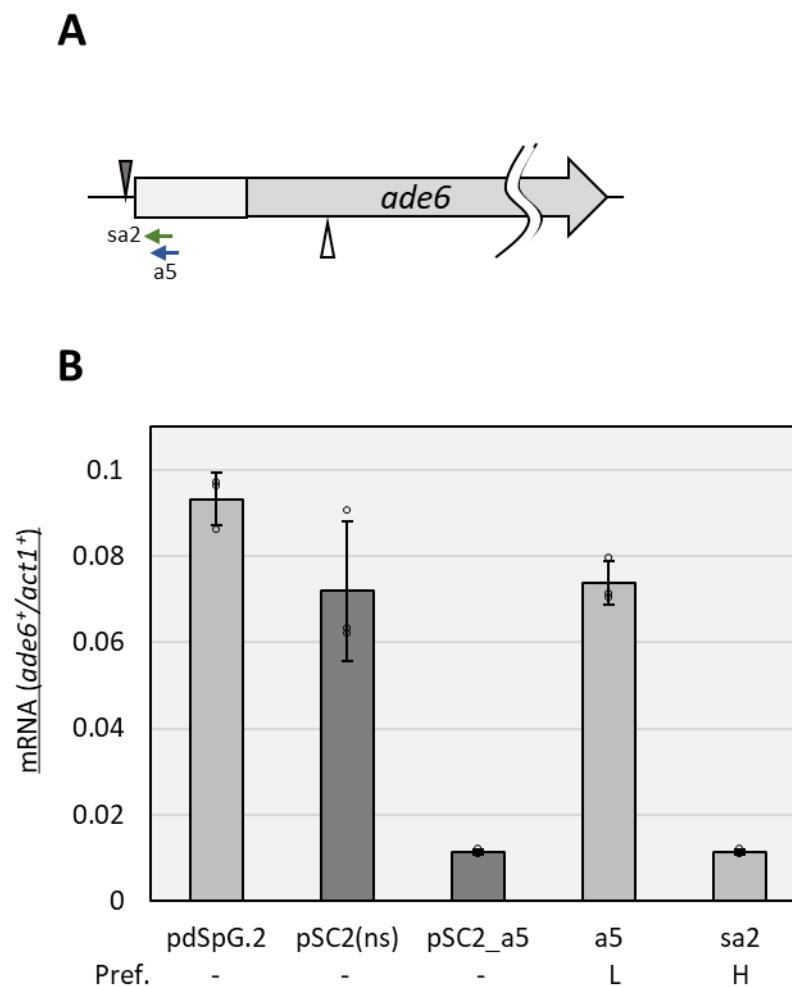


Fig. S1. An example of a targeting sequence that is effective with dCas9, but not with dSpG. (A) Targeting sequences designed for the *ade6*⁺ gene. Arrows indicate targeting sequences of sgRNAs that bind the non-template strand of the targeted DNA. Blue arrow is a targeting sequence suitable for dCas9. The green arrow is suitable for dSpG. PAM sequences are situated at the immediate 3'-side of the arrowheads (not shown in the diagram). A gray triangle indicates the TSS. A white triangle indicates the position of 90 bp downstream from the TSS. A light gray box indicates the 5'UTR. (B) Quantification of *ade6*⁺ mRNA. mRNA of *ade6*⁺ and *act1*⁺ was quantified by RT-qPCR. Relative mRNA amounts of *ade6*⁺ normalized by that of *act1*⁺ are presented. Dark gray bars indicate results of dCas9-mediated methods. Light bars indicate results of dSpG-mediated methods. Data show means +/- standard deviation from three biological replicates. Open circles indicate individual data points. Data of pSC2 (n.s.), pSC2_a5, pdSpG.2, and sa2 are identical to those presented in the main Figure 2.

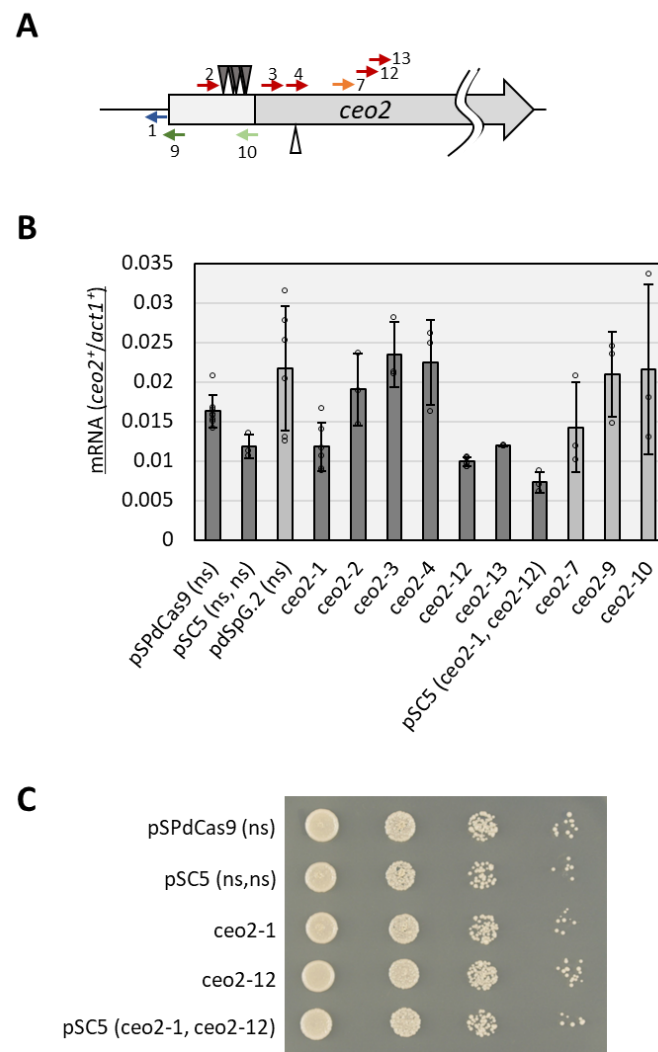


Fig. S2. Knockdown of *ceo2*⁺ using CRISPRi methods.

(A) Targeting sequences designed for the *ceo2*⁺ gene. Red and blue arrows indicate targeting sequences of sgRNAs that base-pair with the template and non-template strand of the targeted DNA respectively for the dCas9-mediated CRISPRi. Orange and green arrows indicate ones for dSpG-mediated CRISPRi (high preference, *ceo2*-9; moderate preference, *ceo2*-10, *ceo2*-7). PAM sequences are situated at the immediate 3'-side of the arrowheads (not shown in the diagram). Gray triangle, TSS; white triangle, the position of 90 bp downstream from the TSS; light gray box, 5'UTR

(B) Quantification of mRNA. mRNA of indicated gene and *act1*⁺ was quantified by RT-qPCR. Relative mRNA amounts of target genes normalized by that of *act1*⁺ are presented. Dark gray bars indicate results of dCas9-mediated methods. Light gray bars indicate results of dSpG-mediated methods. Data show means +/- standard deviation from at least three biological replicates (pSPdCas9 (ns), n = 8; pdSpG.2 (ns), n = 6; *ceo2*-1, n = 6; others, n = 3). ns, nonsense targeting sequence; open circle, individual data point

(C) Serial dilution (10-fold) spot test growth assays of fission yeast cells bearing CRISPRi plasmids with the indicated targeting sequences, on the EMM2 plate.

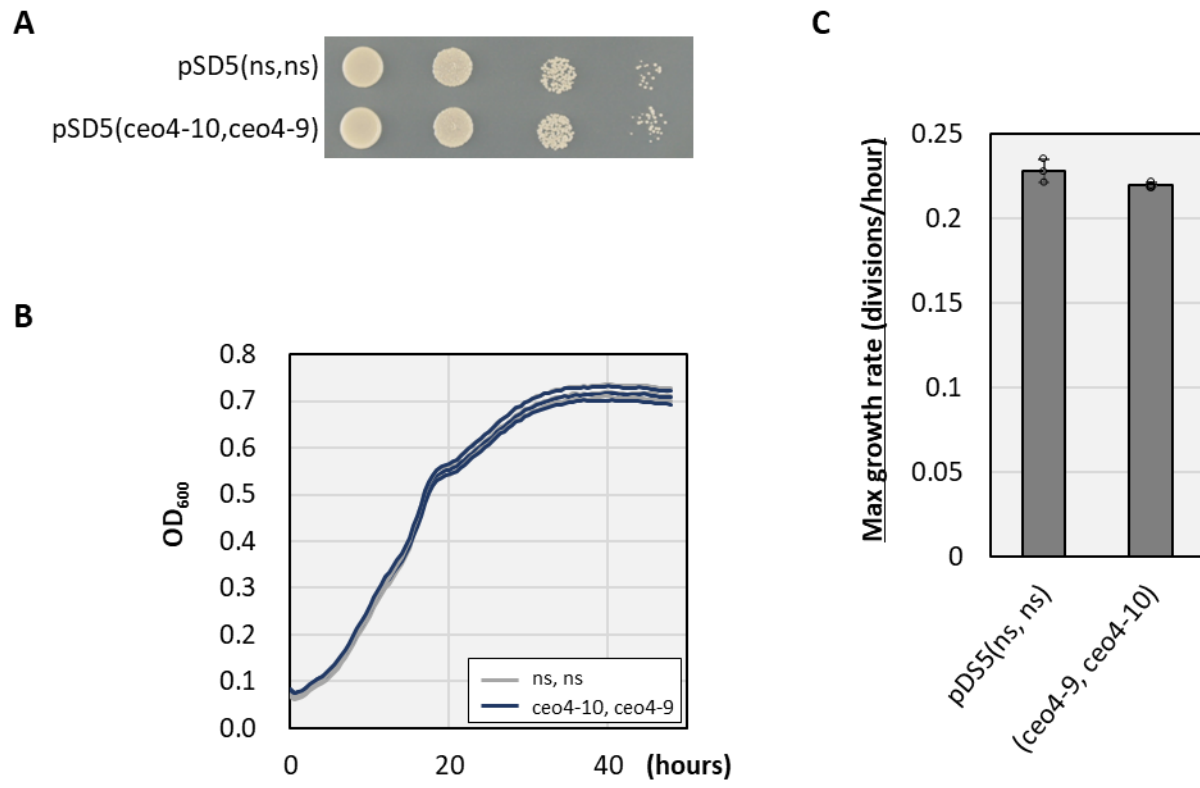


Fig. S3. Growth rate phenotype of the *ceo4*⁺ knockdown strain.

(A) Serial dilution (10-fold) spot test growth assays of fission yeast cells bearing CRISPRi plasmids with the indicated targeting sequences, on an EMM2 plate.

(B) Time course measurement of OD₆₀₀ after CRISPRi induction. Fission yeast cells carrying CRISPRi plasmids were grown in a microplate reader with OD₆₀₀ measurements every 30 min after CRISPRi induction (see Materials and Methods for details). Results of three biological replicates are shown for each strain.

(C) Maximum growth rate (divisions/hour) calculated from results in the panel (B). Results show means +/- standard deviation from three biological replicates. Open circles indicate individual data points.

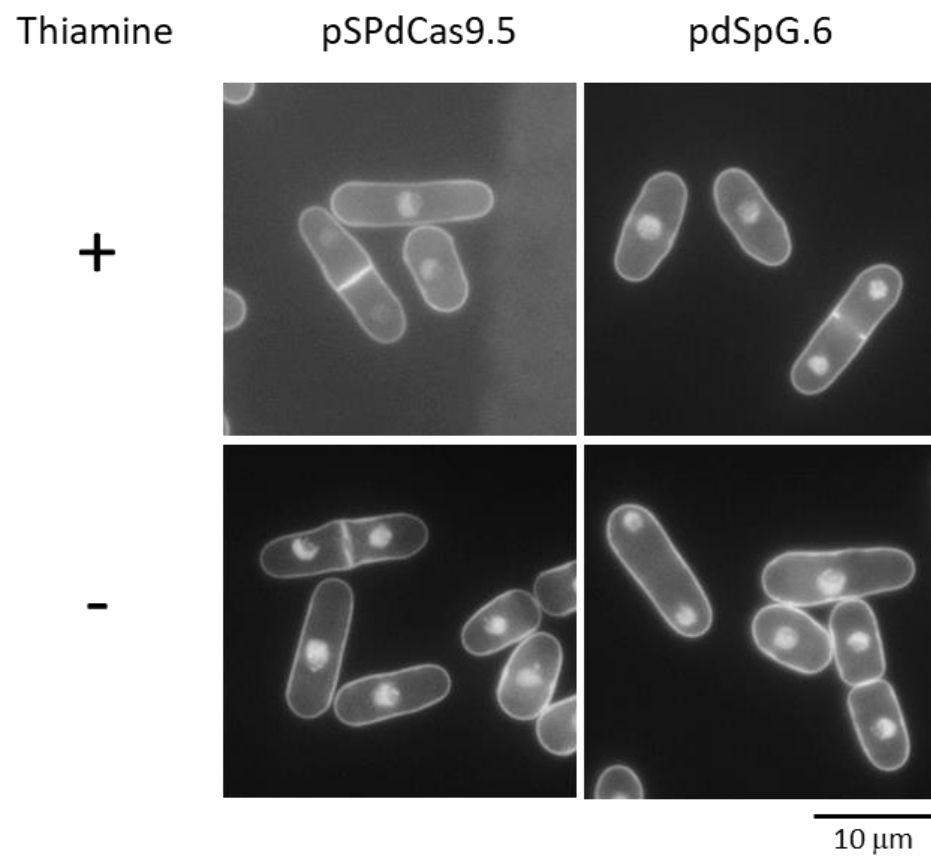


Fig. S4. Cell morphology of control strains for double sgRNA repression.

Fission yeast strains carrying control plasmids pSPdCas9.5 or pdSpG.6 were analyzed for cellular morphology. Fission yeast cells before (thiamine +) and after (thiamine -) 48 h of CRISPRi induction were fixed with 2.5% glutaraldehyde and stained with DAPI, followed by fluorescence microscopy (see Materials and Methods for details). A scale bar indicates 10 μm. The pdSpG.6 plasmid has nonsense targeting sequences of the BbsI cloning site (sgRNA1) and a random sequence (sgRNA2) instead of the PaqCI cloning site. pdSpG.6 was used instead of pdSpG.5, because pdSpG.5 inhibited cell proliferation in culture conditions of this experiment while pdSpG.6 did not affect cell proliferation.

Table S1. human orthologs of *ceo* genes are involved in human health

gene name	human ortholog	essential in human cancer cell lines	human diseases caused by mutation	molecular function	references
<i>ceo1</i>	TMEM97	-	- ^c	cellular cholesterol regulation	Wilcox et al., 2007
<i>ceo2</i>	PPA1, PPA2	KBM7, HAP1, K562, Jioye, Raji ^a	sudden cardiac failure	pyrophosphatase	Curbo et al., 2006 Guimier et al., 2016
<i>ceo3</i>	RDH14	-	intellectual disability, cerebellar atrophy	retinol reductase	Belyaeva et al., 2002 Pastore et al., 2021
<i>ceo4</i>	C2orf76	-	-	-	
<i>ceo5</i>	TTC27	KBM7, HAP1, K562, Jioye, Raji ^a	-	-	
<i>ceo6</i>	NCDN	- ^b	Neurodevelopmental disorder with infantile epileptic spasms	mGluR5 signaling regulation	Wang et al., 2009 Fatima et al., 2021
<i>ceo7</i>	ATXN10	KBM7, HAP1 ^a	spinocerebellar ataxia type 10	-	Matsuura et al., 2000

a, (Wang et al., 2015; Blomen et al., 2015); b, predicted essential gene for humans (Georgi et al., 2013); c, related to cancer malignancy (Wilcox et al., 2007)

Table S2. oligo DNA list

ID	purpose	targeting sequence ID	sequence (5'-)
KI1240	pSPdCas9.3 construction	nonsense (PacCI site)	cacc-TTCAGCAGGTGGACACCTGCCTTA
KI1241	pSPdCas9.3 construction	nonsense (PacCI site)	aaac-TAAGGCAGGTGTCCACCTGCTGAA
KI1169	pSPdCas9.5 construction	NA	cgggatcc-GGCGACCATGGAAATAACTATATCC
KI1248	pSPdCas9.5 construction	NA	CAGGGAAATCATAACATAGTATAATAGGAA
KI1423	pdSpG.2 construction	NA	AAGGACGACTCCATCGACAAC
KI1424	pdSpG.2 construction	NA	AGCTGAGACAGGTCGATCC
KI1425	pdSpG.2 construction	NA	AGAGCATCACCGGCCTGTAC
KI1426	pdSpG.2 construction	NA	TTGTCGCTTCTGGTCAGCAC
KI1024	targeting seq.	a5	cacc-GATGAAGTATGTATATACCT
KI1025	targeting seq.	a5	aaac-AGGTATATACATACTTCATC
KI1046	targeting seq.	a10	cacc-AAACATCAAATGCATCATCT
KI1047	targeting seq.	a10	aaac-AGATGATGCATTTGATGTTT
KI1533	targeting seq.	sa1	cacc-CATTACCATCTCATTAAAGC
KI1534	targeting seq.	sa1	aaac-GCTTAATGAGATGGTAAATG
KI1535	targeting seq.	sa2	cacc-ACCTTGGCAGCTCAGCTTAA
KI1536	targeting seq.	sa2	aaac-TTAAGCTGAGCTGCCAAGGT
KI1537	targeting seq.	sa3	cacc-ATGAAGTATGTATATACCTT
KI1538	targeting seq.	sa3	aaac-AAGGTATATACATACTTCAT
KI1539	targeting seq.	sa4	cacc-TATACATACTTCATCGAATA
KI1540	targeting seq.	sa4	aaac-TATTCGATGAAGTATGTATA
KI1541	targeting seq.	sa5	cacc-CAATTGGGCCGAATGATGGT
KI1542	targeting seq.	sa5	aaac-ACCATCATTCGGCCCAATTG

KI1543	targeting seq.	sa6	cacc-TTGGGCCGAATGATGGTAGA
KI1544	targeting seq.	sa6	aaac-TCTACCATCATTCGGCCCAA
KI1545	targeting seq.	sa7	cacc-CCCATCGCTTAAACATCAAA
KI1546	targeting seq.	sa7	aaac-TTTGATGTTTAAGCGATGGG
KI1547	targeting seq.	sa8	cacc-AACATCAAATGCATCATCTT
KI1548	targeting seq.	sa8	aaac-AAGATGATGCATTTGATGTT
KI1703	targeting seq.	ceo1-9	cacc-ATATCTCACTACTATAAATG
KI1704	targeting seq.	ceo1-9	aaac-CATTTATAGTAGTGAGATAT
KI1705	targeting seq.	ceo1-10	cacc-TCCATGTGAAGGCGTGTGGT
KI1706	targeting seq.	ceo1-10	aaac-ACCACACGCCTTCACATGGA
KI1707	targeting seq.	ceo1-11	cacc-CCTATAACTGAATGGCTTGG
KI1708	targeting seq.	ceo1-11	aaac-CCAAGCCATTCAGTTATAGG
KI1709	targeting seq.	ceo1-12	cacc-GGCTCTTTAAGCTGTCTTTC
KI1710	targeting seq.	ceo1-12	aaac-GAAAGACAGCTTAAAGAGCC
KI1196	targeting seq.	ceo2-1	cacc-TATGAAGTATAAAGCGCTGA
KI1197	targeting seq.	ceo2-1	aaac-TCAGCGCTTTATACTTCATA
KI1198	targeting seq.	ceo2-2	cacc-AGATGGTGTATTACTTTAGT
KI1199	targeting seq.	ceo2-2	aaac-ACTAAAGTAATACACCATCT
KI1200	targeting seq.	ceo2-3	cacc-CAATTTTCGGTCGAAAATCAC
KI1201	targeting seq.	ceo2-3	aaac-GTGATTTTCGACCGAAATTG
KI1202	targeting seq.	ceo2-4	cacc-CACTGGAAAATAAATACGC
KI1203	targeting seq.	ceo2-4	aaac-GCGTATTTAGTTTTCCAGTG
KI1255	targeting seq.	ceo2-7	cacc-AAACCAATTTTCATTCTTCCA
KI1256	targeting seq.	ceo2-7	aaac-TGGAAGAATGAAATTGGTTT
KI1683	targeting seq.	ceo2-9	cacc-TACCACATTATGAAGTATAA
KI1684	targeting seq.	ceo2-9	aaac-TTATACTTCATAATGTGGTA
KI1685	targeting seq.	ceo2-10	cacc-TCATCAATCAACTCTCTAGT
KI1686	targeting seq.	ceo2-10	aaac-ACTAGAGAGTTGATTGATGA
KI2409	targeting seq.	ceo2-12	cacc-TGTCCCATGACATCTGATA
KI2410	targeting seq.	ceo2-12	aaac-TATCAGATGTCAATGGGACA
KI2411	targeting seq.	ceo2-13	cacc-TGATAAGGACACATTTAATA
KI2412	targeting seq.	ceo2-13	aaac-TATTAAATGTGTCCTTATCA

KI1265	targeting seq.	ceo3-1	cacc-GCTACATAACCACTGACATTG
KI1266	targeting seq.	ceo3-1	aaac-CAATGTCAGTGGTATGTAGC
KI1267	targeting seq.	ceo3-2	cacc-CTGTTGATGGAGTTGGCAAA
KI1268	targeting seq.	ceo3-2	aaac-TTTGCCAACTCCATCAACAG
KI1269	targeting seq.	ceo3-3	cacc-GATTGCGGTTTCAACAATTG
KI1270	targeting seq.	ceo3-3	aaac-CAATTGTTGAAACCGCAATC
KI1271	targeting seq.	ceo3-4	cacc-CAATTGCGGCCTTTAAATTC
KI1272	targeting seq.	ceo3-4	aaac-GAATTTAAAGGCCGCAATTG
KI2413	targeting seq.	ceo3-5	cacc-ATGAGCATCTAATTACACAT
KI2414	targeting seq.	ceo3-5	aaac-ATGTGTAATTAGATGCTCAT
KI1655	targeting seq.	ceo4-5	cacc-TGATTGAGATGTGCACTAAG
KI1656	targeting seq.	ceo4-5	aaac-CTTAGTGCACATCTCAATCA
KI1657	targeting seq.	ceo4-6	cacc-TAAGCATAAAGGTGAGGCTC
KI1658	targeting seq.	ceo4-6	aaac-GAGCCTCACCTTTATGCTTA
KI1693	targeting seq.	ceo4-7	cacc-TTGATTAACACTCGAGTCAA
KI1694	targeting seq.	ceo4-7	aaac-TTGA CTGAGTGTTAATCAA
KI1695	targeting seq.	ceo4-8	cacc-AATGGTAACTTGTGTAGTAT
KI1696	targeting seq.	ceo4-8	aaac-ATACTACACAAGTTACCATT
KI1697	targeting seq.	ceo4-9	cacc-CACTCGAGTCAATGGTAACT
KI1698	targeting seq.	ceo4-9	aaac-AGTTACCATTGACTCGAGTG
KI1699	targeting seq.	ceo4-10	cacc-AAGCATAAAGGTGAGGCTCT
KI1700	targeting seq.	ceo4-10	aaac-AGAGCCTCACCTTTATGCTT
KI1701	targeting seq.	ceo4-11	cacc-AACGAAGCATTATAAATGAT
KI1702	targeting seq.	ceo4-11	aaac-ATCATTTATAATGCTTCGTT
KI1188	targeting seq.	ceo5-1	cacc-AGGAATTGAAGATTGGAGTT
KI1189	targeting seq.	ceo5-1	aaac-AACTCCAATCTTCAATTCTT
KI1190	targeting seq.	ceo5-2	cacc-CAGGAATTGAAGATTGGAGT
KI1191	targeting seq.	ceo5-2	aaac-ACTCCAATCTTCAATTCCTG
KI1192	targeting seq.	ceo5-3	cacc-CAGAAATCCACTATTAGAC
KI1193	targeting seq.	ceo5-3	aaac-GTCTAATAGTGGAATTTCTG
KI1194	targeting seq.	ceo5-4	cacc-AGACGGGATAAATGCTTAAT
KI1195	targeting seq.	ceo5-4	aaac-ATTAAGCATTATCCCGTCT

KI1257	targeting seq.	ceo6-1	cacc-CCGCTTATGCTGAGGCAAAA
KI1258	targeting seq.	ceo6-1	aaac-TTTTGCCTCAGCATAAGCGG
KI1261	targeting seq.	ceo6-3	cacc-TGAGTGGAATTTGAGGAAAA
KI1262	targeting seq.	ceo6-3	aaac-TTTTCCTCAAATTCCACTCA
KI1263	targeting seq.	ceo6-4	cacc-GAGGAAAAAGGTGAGAAGTT
KI1264	targeting seq.	ceo6-4	aaac-AACTTCTCACCTTTTTCTC
KI2415	targeting seq.	ceo6-5	cacc-TTTAATTAATCAAGAAAAAT
KI2416	targeting seq.	ceo6-5	aaac-ATTTTTCTTGATTAATTA
KI2417	targeting seq.	ceo6-6	cacc-AAGTAGAAACATTTTTTTTC
KI2418	targeting seq.	ceo6-6	aaac-GAAAAAAAATGTTTCTACT
KI1289	targeting seq.	ceo7-1	cacc-AGTATGTGTCGCAATATGGT
KI1290	targeting seq.	ceo7-1	aaac-ACCATATTGCGACACATACT
KI1291	targeting seq.	ceo7-2	cacc-ACATAGTATGTGTCGCAATA
KI1292	targeting seq.	ceo7-2	aaac-TATTGCGACACATACTATGT
KI1667	targeting seq.	ceo7-5	cacc-TACCTTCAAATAATTTGGGA
KI1668	targeting seq.	ceo7-5	aaac-TCCCAAATTATTTGAAGGTA
KI1689	targeting seq.	ceo7-6	cacc-ACAGAAGCAATGAAGGCTTA
KI1690	targeting seq.	ceo7-6	aaac-TAAGCCTTCATTGCTTCTGT
KI1691	targeting seq.	ceo7-7	cacc-AAATGGAATCAACTGAAGAA
KI1692	targeting seq.	ceo7-7	aaac-TTCTTCAGTTGATTCCATTT
KI915	qPCR (ade6)	NA	GGCGCTGGTATATATGGTGTAG
KI916	qPCR (ade6)	NA	ATGGTGTAGTGACCTGAATTGT
act1-Fw	qPCR (act1)	NA	CTTTCTACAACGAGCTTCGTGTTG
act1-Rv	qPCR (act1)	NA	GAGTCATCTTCTCACGGTTGGAT
KI1681	qPCR (ceo1)	NA	GGAGGCTCTTTAAGCTGTCTTT
KI1682	qPCR (ceo1)	NA	CCAAGGCGCAGGGATTAAA
KI1226	qPCR (ceo2)	NA	CGAGACTGGTTTGCCATTTAC
KI1227	qPCR (ceo2)	NA	GCTATTATGTCCAACGCATCAC
KI1335	qPCR (ceo3)	NA	ACTCAACCCGTCCTTGTAAT
KI1336	qPCR (ceo3)	NA	CTTCATCAATTTGGGCATCGG
KI1675	qPCR (ceo4)	NA	CGATGAACGCATACAAACGG
KI1676	qPCR (ceo4)	NA	AGAATCCAATCATCGTGGTCTAA

KI1222	qPCR (ceo5)	NA	AGACTGTTGAGGGAGCTTTG
KI1223	qPCR (ceo5)	NA	GACCACACCACCCATTCTT
KI1331	qPCR (ceo6)	NA	ATTAGCGTTGCTCTCCCTTC
KI1332	qPCR (ceo6)	NA	TCGTCATAAACAACTTTCCATGC
KI1341	qPCR (ceo7)	NA	TTAGTACTGCACCTGACTTGG
KI1342	qPCR (ceo7)	NA	GAGATTCGCGGATATACGGATT
KI2995	nonsense control	random sequence 1	cacc-TCTGGATTGACTCTATGACG
KI2996	nonsense control	random sequence 1	aaac-CGTCATAGAGTCAATCCAGA

Table S3. plasmids list

ID	vector	targeting sequence ID (sgRNA2)	targeting sequence ID (sgRNA1)	CRISPRi effector	reference	comment
pSPdCas9	NA	No sgRNA2	nonsense (BbsI site)	dCas9	Ishikawa, <i>G3</i> , 2021	Figure 1A
pSPdCas9.2	NA	No sgRNA2	nonsense (BbsI site)	dCas9	This work	Figure 1A (A cloning site is inserted at the SbfI site)
pSPdCas9.3	NA	No sgRNA2	nonsense (PacCI site)	dCas9	This work	See materials and methods section.
pSPdCas9.5	NA	nonsense (PacCI site)	nonsense (BbsI site)	dCas9	This work	Figure 1B
pdSpG.2	NA	No sgRNA2	nonsense (BbsI site)	dSpG	This work	Figure 1C
pdSpG.5	NA	nonsense (PacCI site)	nonsense (BbsI site)	dSpG	This work	Figure 1D
pDC2_a5	pSPdCas9.2	No sgRNA2	a5	dCas9	This work	Figure 2
pDC2_a10	pSPdCas9.2	No sgRNA2	a10	dCas9	This work	Figure 2
pSC5(a5, ns)	pSPdCas9.5	a5	nonsense (BbsI site)	dCas9	This work	Figure 2
pSC5(ns, a5)	pSPdCas9.5	nonsense (PacCI site)	a5	dCas9	This work	Figure 2
pSC5(a5, a10)	pSPdCas9.5	a5	a10	dCas9	This work	Figure 2

pSC5(a10, a5)	pSPdCas9.5	a10	a5	dCas9	This work	Figure 2
pDS_sa1	pdSpG.2	No sgRNA2	sa1	dSpG	This work	Figure 2
pDS_sa2	pdSpG.2	No sgRNA2	sa2	dSpG	This work	Figure 2
pDS_sa3	pdSpG.2	No sgRNA2	sa3	dSpG	This work	Figure 2
pDS_sa4	pdSpG.2	No sgRNA2	sa4	dSpG	This work	Figure 2
pDS_sa5	pdSpG.2	No sgRNA2	sa5	dSpG	This work	Figure 2
pDS_sa6	pdSpG.2	No sgRNA2	sa6	dSpG	This work	Figure 2
pDS_sa7	pdSpG.2	No sgRNA2	sa7	dSpG	This work	Figure 2
pDS_sa8	pdSpG.2	No sgRNA2	sa8	dSpG	This work	Figure 2
pDC_ceo3-1	pSPdCas9	No sgRNA2	ceo3-1	dCas9	This work	Figure 3
pDC_ceo3-2	pSPdCas9	No sgRNA2	ceo3-2	dCas9	This work	Figure 3
pDC_ceo3-3	pSPdCas9	No sgRNA2	ceo3-3	dCas9	This work	Figure 3
pDC_ceo3-4	pSPdCas9	No sgRNA2	ceo3-4	dCas9	This work	Figure 3
pDC_ceo3-5	pSPdCas9	No sgRNA2	ceo3-5	dCas9	This work	Figure 3
pDC_ceo5-1	pSPdCas9	No sgRNA2	ceo5-1	dCas9	This work	Figure 3
pDC_ceo5-2	pSPdCas9	No sgRNA2	ceo5-2	dCas9	This work	Figure 3
pDC_ceo5-3	pSPdCas9	No sgRNA2	ceo5-3	dCas9	This work	Figure 3
pDC_ceo5-4	pSPdCas9	No sgRNA2	ceo5-4	dCas9	This work	Figure 3
pDC_ceo7-1	pSPdCas9	No sgRNA2	ceo7-1	dCas9	This work	Figure 3
pDC_ceo7-2	pSPdCas9	No sgRNA2	ceo7-2	dCas9	This work	Figure 3
pDC_ceo7-5	pSPdCas9	No sgRNA2	ceo7-5	dCas9	This work	Figure 3
pDC_ceo7-6	pSPdCas9	No sgRNA2	ceo7-6	dCas9	This work	Figure 3
pDC_ceo7-7	pSPdCas9	No sgRNA2	ceo7-7	dCas9	This work	Figure 3

pDC_ ceo6-1	pSPdCas9	No sgRNA2	ceo6-1	dCas9	This work	Figure 4
pDC_ ceo6-3	pSPdCas9	No sgRNA2	ceo6-3	dCas9	This work	Figure 4
pDC_ ceo6-4	pSPdCas9	No sgRNA2	ceo6-4	dCas9	This work	Figure 4
pDC_ ceo6-5	pSPdCas9	No sgRNA2	ceo6-5	dCas9	This work	Figure 4
pDC_ ceo6-6	pSPdCas9	No sgRNA2	ceo6-6	dCas9	This work	Figure 4
pSC5(ceo6-1, ceo6-3)	pSPdCas9.5	ceo6-1	ceo6-3	dCas9	This work	Figure 4
pDC_ ceo1-9	pSPdCas9	No sgRNA2	ceo1-9	dCas9	This work	Figure 4
pDC_ ceo1-10	pSPdCas9	No sgRNA2	ceo1-10	dCas9	This work	Figure 4
pDC_ ceo1-11	pSPdCas9	No sgRNA2	ceo1-11	dCas9	This work	Figure 4
pDC_ ceo1-12	pSPdCas9	No sgRNA2	ceo1-12	dCas9	This work	Figure 4
pSC5(ceo1-9, ceo1-12)	pSPdCas9.5	ceo1-9	ceo1-12	dCas9	This work	Figure 4
pDC_ ceo4-5	pSPdCas9	No sgRNA2	ceo4-5	dCas9	This work	Figure 5
pDC_ ceo4-6	pSPdCas9	No sgRNA2	ceo4-6	dCas9	This work	Figure 5
pDC_ ceo4-7	pSPdCas9	No sgRNA2	ceo4-7	dCas9	This work	Figure 5
pDS_ ceo4-8	pSPdCas9	No sgRNA2	ceo4-8	dSpG	This work	Figure 5
pDS_ ceo4-9	pdSpG.2	No sgRNA2	ceo4-9	dSpG	This work	Figure 5
pDS_ ceo4-10	pdSpG.2	No sgRNA2	ceo4-10	dSpG	This work	Figure 5
pDS_ ceo4-11	pdSpG.2	No sgRNA2	ceo4-11	dSpG	This work	Figure 5
pDS5(ceo4-10, ceo4-9)	pdSpG.5	ceo4-10	ceo4-9	dSpG	This work	Figure 5
pDS_ a5	pdSpG.2	No sgRNA2	a5	dSpG	This work	Figure S1
pDC_ ceo2-1	pSPdCas9	No sgRNA2	ceo2-1	dCas9	This work	Figure S2
pDC_ ceo2-2	pSPdCas9	No sgRNA2	ceo2-2	dCas9	This work	Figure S2
pDC_ ceo2-3	pSPdCas9	No sgRNA2	ceo2-3	dCas9	This work	Figure S2
pDC_ ceo2-4	pSPdCas9	No sgRNA2	ceo2-4	dCas9	This work	Figure S2
pDC_ ceo2-12	pSPdCas9	No sgRNA2	ceo2-12	dCas9	This work	Figure S2
pDC_ ceo2-13	pSPdCas9	No sgRNA2	ceo2-13	dCas9	This work	Figure S2
pDS_ ceo2-7	pdSpG.2	No sgRNA2	ceo2-7	dSpG	This work	Figure S2
pDS_ ceo2-9	pdSpG.2	No sgRNA2	ceo2-9	dSpG	This work	Figure S2
pDS_ ceo2-10	pdSpG.2	No sgRNA2	ceo2-10	dSpG	This work	Figure S2
pSC5(ceo2-1, ceo2-12)	pSPdCas9.5	ceo2-1	ceo2-12	dCas9	This work	Figure S2
pdSpG.6	pdSpG.5	nonsense (random sequence 1)	nonsense (BbsI site)	dSpG	This work	Figure S4